© 2015. Published by The Company of Biologists Ltd | Journal of Cell Science (2015) 128, 1034–1050 doi:10.1242/jcs.162552

RESEARCH ARTICLE

The heterotrimeric kinesin-2 complex interacts with and regulates GLI protein function

Brandon S. Carpenter, Renee L. Barry, Kristen J. Verhey and Benjamin L. Allen*

ABSTRACT

GLI transport to the primary cilium and nucleus is required for proper Hedgehog (HH) signaling; however, the mechanisms that mediate these trafficking events are poorly understood. Kinesin-2 motor proteins regulate ciliary transport of cargo, yet their role in GLI protein function remains unexplored. To examine a role for the heterotrimeric KIF3A–KIF3B–KAP3 kinesin-2 motor complex in regulating GLI activity, we performed a series of structure-function analyses using biochemical, cell signaling and *in vivo* approaches that define novel specific interactions between GLI proteins and two components of this complex, KAP3 and KIF3A. We find that all three mammalian GLI proteins interact with KAP3 and we map specific interaction sites in both proteins. Furthermore, we find that GLI proteins interact selectively with KIF3A, but not KIF3B, and that GLI interacts synergistically with KAP3 and KIF3A. Using a combination of cell signaling assays and chicken *in ovo* electroporation, we demonstrate that KAP3 interactions restrict GLI activator function but not GLI repressor function. These data suggest that GLI interactions with KIF3A–KIF3B–KAP3 complexes are essential for proper GLI transcriptional activity.

KEY WORDS: Hedgehog, GLI, KAP3, Kinesin-2, KIF3

INTRODUCTION

Hedgehog (HH) signaling is an evolutionarily conserved pathway that is indispensable for embryonic development and also functions in adult tissue homeostasis, renewal and regeneration (reviewed in McMahon et al., 2003; Briscoe and Thérond, 2013). Vertebrate HH signaling initiates when secreted HH ligands bind to the twelve-pass transmembrane receptor Patched (PTCH1) (Stone et al., 1996; Marigo et al., 1996) and to the co-receptors GAS1, CDON and BOC (Allen et al., 2011); this relieves inhibition of Smoothened (SMO), a seven-pass transmembrane G-protein-coupled receptor (GPCR)-like protein that initiates a signal transduction cascade culminating in modulation of the GLI family of zinc-finger transcription factors (GLI1–3) (Hui and Angers, 2011). As effector molecules of the HH pathway, GLI proteins act in the nucleus to both activate and repress HH target gene expression (Ruiz i Altaba, 2011; Sasaki et al., 1999; Stamataki et al., 2005; Vokes et al., 2007).

There are three mammalian GLI proteins – GLI1, which functions exclusively as a transcriptional activator and is dispensable for mammalian development (Bai et al., 2002), GLI2, the main transcriptional activator of the HH pathway (Ding et al., 1998; Bai et al., 2002), and GLI3, which acts primarily as a transcriptional repressor (Altaba, 1999; Bai et al., 2004). GLI2 and GLI3 both contain N-terminal repressor and C-terminal activation domains that regulate their function (Sasaki et al., 1999; Aza-Blanc et al., 2000; Stamataki et al., 2005). In the absence of HH signaling, GLI2 and GLI3 are proteolytically processed into N-terminal repressors that inhibit HH target gene transcription (Wang et al., 2000). Conversely, HH ligand stimulation promotes the accumulation of full-length GLI2 and GLI3 that activate HH target gene transcription (Pan et al., 2006).

Recent studies indicate a significant role for primary cilia in the regulation of GLI protein processing and function (reviewed by Nozawa et al., 2013). GLI2 and GLI3 constitutively traffic through primary cilia at low levels (Haycraft et al., 2005; Norman et al., 2009), and activation of the HH pathway promotes GLI2 and GLI3 accumulation at the tips of primary cilia (Endoh-Yamagami et al., 2009; Wen et al., 2010); this correlates with the accumulation of full-length GLI proteins that activate HH target gene transcription. Notably, all mammalian GLI proteins traffic to primary cilia (Haycraft et al., 2005), and disruption of ciliogenesis affects both the processing and function of GLI2 and GLI3, which results in defects in digit formation and neural tube patterning (Haycraft et al., 2005; Liu et al., 2005). Despite their implication in GLI protein regulation, the mechanisms by which primary cilia regulate GLI activity and processing are not well understood.

Intraflagellar transport (IFT) complexes are responsible for cilia formation and maintenance, and for the trafficking of cargo within primary cilia (reviewed by Pedersen and Rosenbaum, 2008). These complexes consist of IFT particles (A and B) that are trafficked along microtubule-based axonemes by anterograde (kinesin-2) and retrograde (dynein) motor proteins (reviewed by Goetz and Anderson, 2010). Roles for these various IFT components in GLI protein ciliary trafficking are starting to emerge. For example, mutations in genes that encode components of retrograde motors (*Dync2h1*), IFT A complexes (*Ift122*), or IFT B complexes (*Ift25*, also known as *Hspb11*) cause GLI protein mislocalization at ciliary tips that correlates with aberrant HH signaling (Ocbina et al., 2011; Qin et al., 2011; Keady et al., 2012). Although these studies indicate a role for IFT particles and retrograde motors in GLI processing and function, the mechanisms of how GLI proteins are trafficked within and between subcellular compartments remains largely unexplored.

One outstanding question is: what regulates the intracellular trafficking of GLI proteins between the cytoplasm, nucleus and primary cilium? The KIF3A–KIF3B–KAP3 heterotrimeric complex is an evolutionarily conserved kinesin-2 motor that mediates plus-end-directed protein transport along microtubules and plays important functional roles in both ciliary and

Department of Cell and Developmental Biology, University of Michigan, Ann Arbor, MI 48109, USA.

*Author for correspondence (benallen@umich.edu)

Received 28 August 2014; Accepted 19 December 2014

Journal of Cell Science

Journal of Cell Science (2015) 128, 1034–1050 doi:10.1242/jcs.162552

intracellular transport (reviewed by Scholey, 2013; Cole et al., 1993; Wedaman et al., 1996). Mutations in *Kif3a*, *Kif3b* or the non-motor component, kinesin-associated protein (*Kifap3*; referred to hereafter as *Kap3*) cause ciliary defects that lead to mid-gestation lethality and randomization in left-right asymmetry (Takeda et al., 1999; Hirokawa, 2000; Nonaka et al., 1998). Mice lacking KIF3A also display aberrant neural tube patterning similar to phenotypes seen in mice containing mutations that prevent HH pathway activation (Huangfu et al., 2003). Previous work in vertebrates identified KAP3 as an armadillo repeat-containing protein that forms a heterotrimeric complex with KIF3A and KIF3B and scaffolds cargo to the motors (Yamazaki et al., 1995; 1996). Similar to *Kif3a* and *Kif3b* mutant mice, *Kap3* mutant mice die during mid-gestation (Teng et al., 2005), owing to the central role of the heterotrimeric kinesin-2 complex in ciliogenesis (reviewed in Scholey, 2013). Further, it is this crucial role for KIF3A, KIF3B and KAP3 in ciliogenesis that complicates the use of genetics to address their role in HH signaling and explains why a role for these molecules in regulating GLI protein activity has remained elusive.

In order to dissect the role of the KIF3A–KIF3B–KAP3 complex in directly regulating GLI protein trafficking and function independent of its role in ciliogenesis, we employed a combination of biochemical, cell signaling and *in vivo* approaches to define novel interactions between GLI proteins and members of the kinesin-2 motor complex. Specifically, we demonstrate that both KAP3 and KIF3A, but not KIF3B, interact with GLI proteins, and we map the site of these interactions between all three proteins. Furthermore, using cell signaling assays and chicken *in ovo* electroporation, we find that KAP3 restricts GLI activator function but not GLI repressor function. Taken together, these data identify novel selective physical interactions between kinesin-2 motor complex components that specifically regulate GLI protein function.

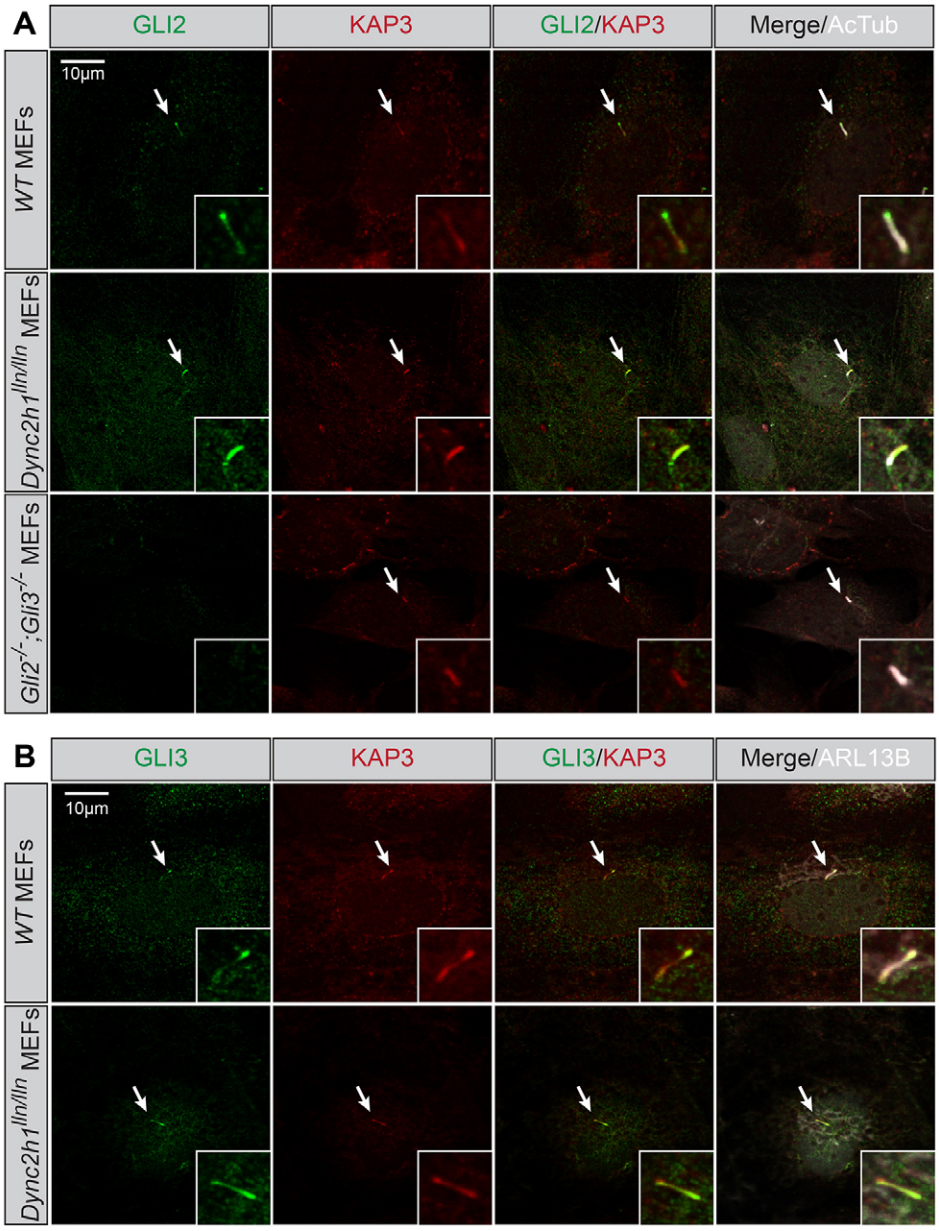

Fig. 1. Endogenous KAP3 and GLI proteins localize to primary cilia. (A) Antibody detection of endogenous GLI2 (green) and KAP3 (red) in wild-type (WT, upper row), *Dync2h1*$^{lln/lln}$ (middle row) or *Gli2*$^{-/-}$;*Gli3*$^{-/-}$ MEFs (lower row). Primary cilia are identified with antibodies against acetylated tubulin (AcTub; gray). (B) Antibody detection of endogenous GLI3 (green) and KAP3 (red) in wild-type (upper row) and *Dync2h1*$^{lln/lln}$ MEFs (lower row). Primary cilia are identified with antibodies against ARL13B (gray). Arrows denote localization of KAP3A and GLI2 or GLI3 in primary cilia. Insets show areas of interest at higher magnification.

Journal of Cell Science (2015) 128, 1034–1050 doi:10.1242/jcs.162552

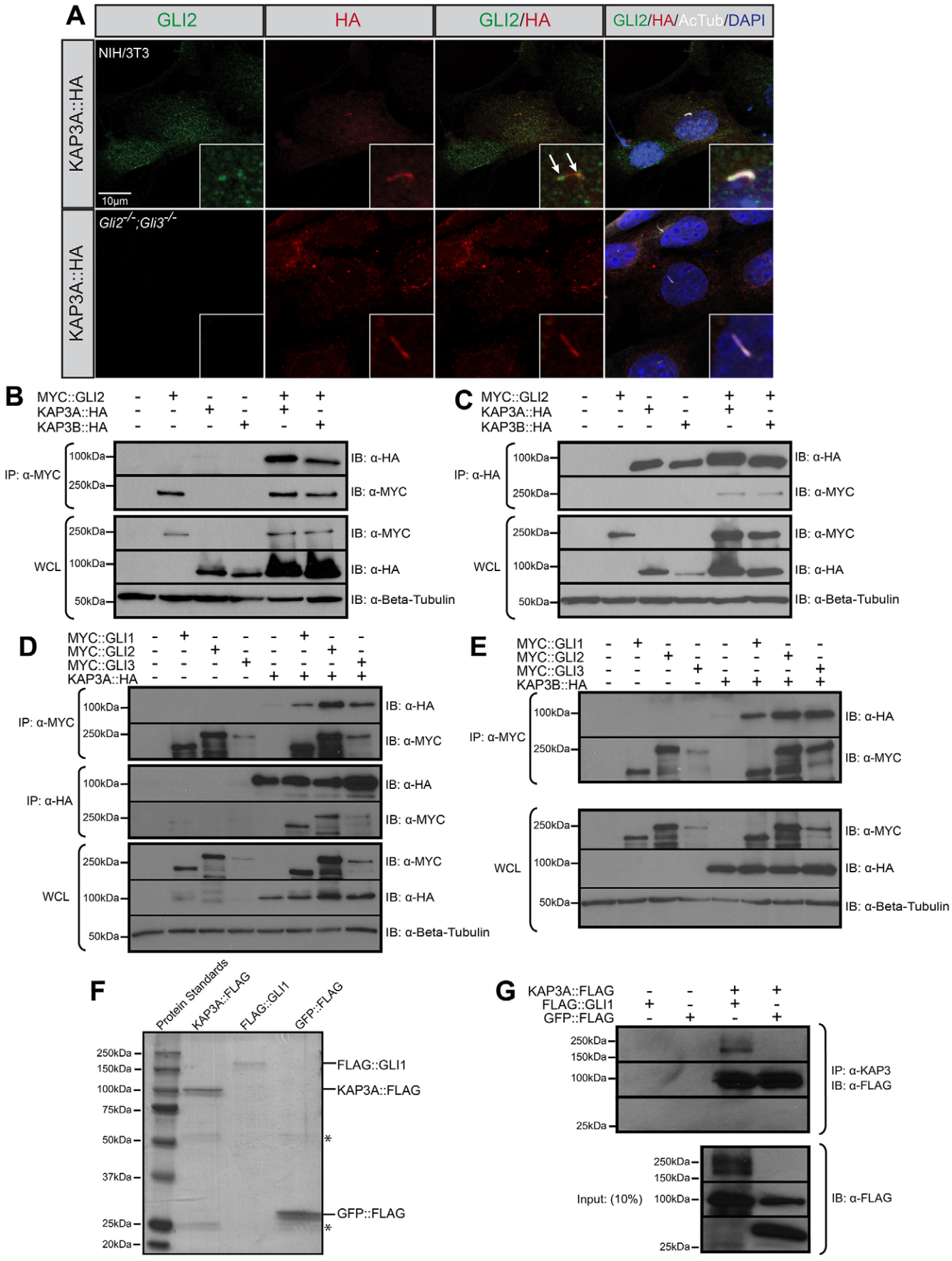

Fig. 2. See next page for legend.

Fig. 2. KAP3 localizes and interacts with mammalian GLI proteins. (A) Antibody detection of endogenous GLI2 in NIH/3T3 cells (upper row; green) or *Gli2*$^{-/-}$;*Gli3*$^{-/-}$ MEFs (lower row; green) expressing HA-tagged KAP3A (KAP3::HA; red). Primary cilia are identified using antibodies directed against acetylated tubulin (AcTub; gray). DAPI denotes nuclei (blue). Insets represent high-magnification images of primary cilia. Arrows denote colocalization of KAP3A and GLI2 in primary cilia. (B) Immunoprecipitation of MYC-tagged GLI2 (MYC::GLI2) from COS-7 cells expressing either HA-tagged KAP3A (KAP3A::HA) or KAP3B (KAP3B::HA). (C) Immunoprecipitation of KAP3A::HA or KAP3B::HA from COS-7 cells co-expressing MYC::GLI2. (D) Immunoprecipitation of MYC::GLI1-3 or KAP3A::HA from COS-7 cells co-expressing MYC::GLI1-3 and/or KAP3A::HA. (E) Immunoprecipitation of MYC::GLI1-3 from COS-7 cells co-expressing MYC::GLI1-3 and/or KAP3B::HA. Immunoprecipitates (IP) and whole-cell lysates (WCL) were subjected to SDS-PAGE and western blot analysis (IB) using antibodies directed against MYC (α-MYC) and HA (α-HA). Antibody detection of β-tubulin (α-Beta-Tubulin) was used to confirm equal loading across lanes. (F) Gel Code Blue detection of affinity-purified KAP3A::FLAG, FLAG::GLI1 and GFP::FLAG from COS-7 cell lysates. Asterisks (*) denote FLAG antibody heavy and light chains eluted from the FLAG–agarose beads. (G) Immunoprecipitation (upper blots) of purified KAP3A::FLAG using an endogenous KAP3 antibody (IP: α-KAP3) followed by western blot analysis with anti-FLAG antibody (IB: α-FLAG) to detect KAP3A::FLAG, FLAG::GLI1 or GFP::FLAG. 10% of the inputs (lower blots) were visualized by western blot analysis to confirm equal protein levels. The molecular masses (in kDa) of protein standards are indicated at the left of each blot.

RESULTS

KAP3 localizes with GLI2 and GLI3 in different subcellular compartments

To determine whether the heterotrimeric KIF3A–KIF3B–KAP3 complex colocalizes with GLI proteins, we initially compared the distribution of endogenous GLI2 and GLI3 with that of endogenous KAP3 in mouse embryonic fibroblasts (MEFs) (Fig. 1). In wild-type MEFs, both GLI2 and GLI3 localized to multiple subcellular compartments, including the nucleus, cytoplasm and the tips of primary cilia (Fig. 1A,B, upper rows). Similar to GLI2 and GLI3, KAP3 localized to multiple subcellular compartments and colocalized with GLI2 and GLI3 within the tips of primary cilia (Fig. 1A,B, upper rows, white arrows). Whereas GLI2 and GLI3 colocalized with KAP3 largely at the tips of primary cilia in wild-type MEFs, colocalization was observed along the entire length of cilia in *Dync2h1* mutant MEFs that are defective in retrograde ciliary trafficking (Fig. 1A, middle row; Fig. 1B, lower row; Ocbina et al., 2011). Furthermore, KAP3 localized to primary cilia in *Gli2*$^{-/-}$;*Gli3*$^{-/-}$ MEFs, suggesting that endogenous KAP3 ciliary localization is independent of GLI2 and GLI3 (Fig. 1A, lower row).

In addition to assessing endogenous colocalization, we also compared the distribution of endogenous GLI2 and GLI3 with epitope-tagged KAP3A (KAP3A::HA) in HH-responsive NIH/3T3 fibroblasts (Fig. 2; supplementary material Fig. S1). Similar to what we observed in MEFs, endogenous GLI2 and GLI3 localized to multiple subcellular compartments, including the cytoplasm, nucleus and primary cilium (Fig. 2A; supplementary material Fig. S1A, upper row). Similarly, KAP3A::HA localized to multiple subcellular compartments and colocalized with endogenous GLI2 and GLI3 in primary cilia (Fig. 2A; supplementary material Fig. S1A, white arrows). More importantly, KAP3A::HA distribution was similar to that of endogenous KAP3, confirming that KAP3A::HA localizes to the same subcellular compartments as endogenous KAP3 (compare Fig. 1A and Fig. 2A).

To confirm the specificity of the endogenous GLI2 and GLI3 antibodies in NIH/3T3 cells and to assess whether KAP3A::HA ciliary localization requires GLI2 and/or GLI3, we examined KAP3A::HA localization in *Gli2*$^{-/-}$;*Gli3*$^{-/-}$ MEFs (Fig. 2A; supplementary material Fig. S1A, lower rows). In *Gli2*$^{-/-}$;*Gli3*$^{-/-}$ MEFs, no GLI2 or GLI3 antibody signal is detected; however, KAP3A::HA still localized to primary cilia (Fig. 2A; supplementary material Fig. S1A, lower rows). These data indicate that, like endogenous KAP3, KAP3A::HA localizes to primary cilia independently of GLI2 and GLI3.

To further assess the colocalization of GLI2 and KAP3A, we expressed an epitope-tagged version of GLI2 (MYC::GLI2) in NIH/3T3 cells (supplementary material Fig. S1B). MYC::GLI2 localized to both the nucleus and cytoplasm, and colocalized with KAP3A::HA in these subcellular compartments (supplementary material Fig. S1B). These data suggest that, in addition to primary cilia, GLI2 can colocalize with KAP3 in the cytoplasm and nucleus when the two proteins are expressed at similar levels.

KAP3A and KAP3B specifically interact with all full-length mammalian GLI proteins

To investigate whether KAP3 proteins physically interact with GLI2, we performed co-immunoprecipitation experiments in COS-7 cells. Two isoforms of mammalian KAP3 exist – KAP3A and KAP3B (Yamazaki et al., 1996). KAP3A is a 792-amino-acid protein containing nine armadillo repeats (Yamazaki et al., 1996). KAP3B is an alternatively spliced isoform of KAP3A that contains a 66-base-pair insertion immediately downstream of the codon for amino acid 757, generating a truncated 772-amino-acid protein (Yamazaki et al., 1996). COS-7 cells were co-transfected with MYC::GLI2 and either KAP3A::HA or KAP3B::HA, followed by immunoprecipitation and western blot analysis (Fig. 2B,C). We found that both KAP3A::HA and KAP3B::HA co-precipitated with MYC::GLI2 (Fig. 2B). Similarly, immunoprecipitation of either KAP3A::HA or KAP3B::HA also co-precipitated MYC::GLI2 (Fig. 2C). Notably, both KAP3A::HA and KAP3B::HA appeared to be stabilized in the presence of GLI2 (Fig. 2B,C, compare KAP3 expression in lysates from cells transfected with KAP3 alone with that in lysates co-transfected with KAP3 and GLI2). By contrast, KAP3A and KAP3B did not interact significantly with the structurally related zinc-finger-containing transcription factor ZIC1 (supplementary material Fig. S2A). Overall, these data suggest that GLI2 specifically interacts with both isoforms of KAP3.

The physical association of GLI2 with KAP3A and KAP3B prompted us to ask whether KAP3A and KAP3B also interact with the other full-length mammalian GLI proteins, namely GLI1 and GLI3. Similar to GLI2, we found that KAP3A co-precipitated with either GLI1 or GLI3 (Fig. 2D, upper panels) and that immunoprecipitation of KAP3A also co-precipitated GLI1 and GLI3 (Fig. 2D, middle panels). We also found that KAP3B co-precipitated with GLI1 and GLI3 (Fig. 2E). Taken together, these data indicate that KAP3A and KAP3B physically interact specifically with all three mammalian GLI proteins.

To determine whether the interaction between GLI and KAP3 proteins is direct, we purified FLAG-tagged GLI1 and FLAG-tagged KAP3A from cell lysates (Fig. 2F) and performed immunoprecipitation experiments using an antibody directed against endogenous KAP3 (Fig. 2G). We found that purified FLAG::GLI1 co-precipitates with purified KAP3A::FLAG (Fig. 2G). By contrast, purified GFP::FLAG did not co-precipitate with KAP3A (Fig. 2G). These results suggest that GLI proteins interact directly and specifically with KAP3.

GLI2 selectively interacts with kinesin-2 motors and synergistically binds KIF3A and KAP3A

The mechanism by which KAP3 facilitates cargo binding as part of the KIF3A–KIF3B motor complex is not well understood, and

Journal of Cell Science (2015) 128, 1034–1050 doi:10.1242/jcs.162552

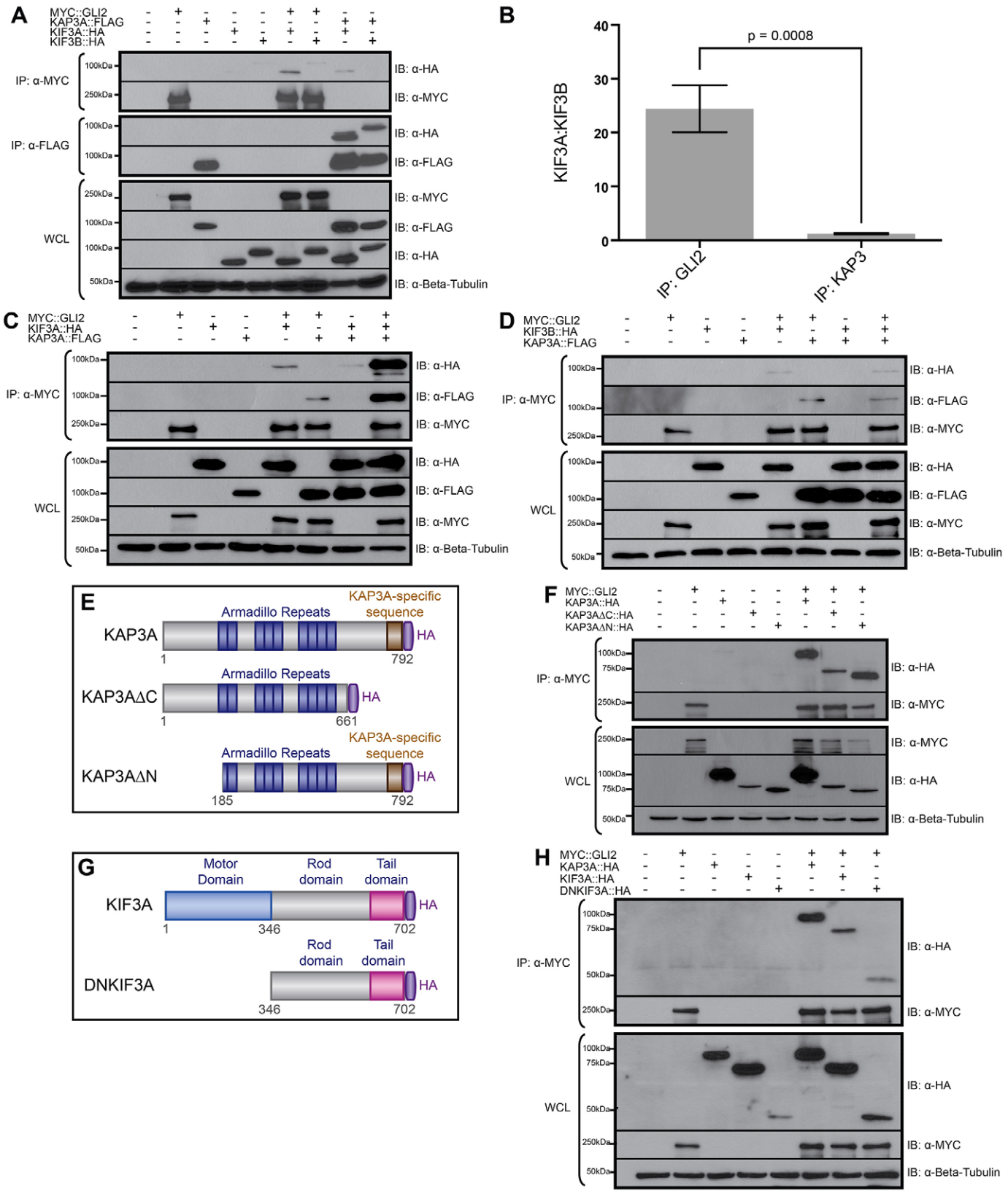

Fig. 3. See next page for legend.

Journal of Cell Science (2015) 128, 1034–1050 doi:10.1242/jcs.162552

Fig. 3. GLI2 selectively interacts with kinesin-2 motors and synergistically binds to the tail domain of KIF3A and the armadillo repeats of KAP3A. (A) Immunoprecipitation of MYC-tagged GLI2 (MYC::GLI2) or FLAG-tagged KAP3A (KAP3A::FLAG) from COS-7 cells expressing HA-tagged KIF3A (KIF3A::HA) or KIF3B (KIF3B::HA). (B) Quantification of the ratio of KIF3A:KIF3B that co-precipitates with either MYC::GLI2 or KAP3A::FLAG. Data show the mean±s.d. of the band densities from three separate experiments; a *P*-value of 0.0008 indicates a significant difference in the KIF3A:KIF3B ratio that co-precipitates with MYC::GLI2 compared with that co-precipitating with KAP3A::FLAG (Student's unpaired *t*-test). (C) Immunoprecipitation of MYC::GLI2 from COS-7 cells expressing KIF3A::HA and/or KAP3A::FLAG. (D) Immunoprecipitation of MYC::GLI2 from COS-7 cells expressing KIF3B::HA and/or KAP3A::FLAG. Immunoprecipitates (IP) and whole-cell lysates (WCL) were subjected to SDS-PAGE and western blot analysis (IB) using antibodies directed against MYC (α-MYC) and HA (α-HA). Antibody detection of β-tubulin (α-Beta-Tubulin) was used to confirm equal loading across lanes. (E) Schematic of full-length and truncated human KAP3A proteins. KAP3A contains highly conserved armadillo repeats (dark blue), a KAP3A-specific sequence (gold) and an HA-tag at the C-terminus (purple). (F) Immunoprecipitation of MYC::GLI2 from COS-7 cells expressing HA-tagged KAP3A (KAP3A::HA), KAP3AΔC (KAP3AΔC::HA) or KAP3AΔN (KAP3AΔN::HA). (G) Schematic of full-length and truncated human KIF3A proteins. KIF3A contains a highly conserved motor domain (blue), a rod domain (gray), a cargo-binding tail domain (pink) and an HA tag at the C-terminus (purple). (H) Immunoprecipitation of MYC::GLI2 from COS-7 cells expressing KAP3A::HA, KIF3A::HA or HA-tagged DNKIF3A (DNKIF3A::HA). Immunoprecipitates and whole-cell lysates were subjected to SDS-PAGE and western blot analysis using antibodies directed against MYC and HA. Antibody detection of β-tubulin was used to confirm equal loading across lanes. The molecular masses (in kDa) of protein standards are indicated at the left of each blot.

whether this complex is involved in transport of the GLI proteins has yet to be addressed. Previous work has indicated that KIF3A–KIF3B can exist as a separate heterodimeric complex that can bind cargo in the absence of KAP3 (Huang et al., 2012; Yamazaki et al., 1995; Yamazaki et al., 1996), suggesting that kinesin-2 motors might use multiple mechanisms to associate with cargo. To test whether KIF3A and KIF3B themselves can interact with GLI proteins, we performed immunoprecipitation studies in COS-7 cells transfected with MYC::GLI2 and either KIF3A::HA or KIF3B::HA (Fig. 3A). As a control, we performed similar experiments in COS-7 cells expressing KAP3A::FLAG and either KIF3A::HA or KIF3B::HA (Fig. 3A).

Surprisingly, immunoprecipitation of GLI2 co-precipitated KIF3A, but not KIF3B (Fig. 3A, upper panels). By contrast, both KIF3A and KIF3B co-precipitated with KAP3 (Fig. 3A, middle panels). Importantly, KIF3A and KIF3B were expressed at equal levels in cell lysates, indicating that protein expression is not an explanation for this discrepancy (Fig. 3A, lower panels). Quantification of these interactions over three separate experiments indicated that nearly 25 times as much KIF3A precipitated with GLI2 compared with that precipitating with KIF3B (Fig. 3B), whereas relatively equal amounts of KIF3A and KIF3B interacted with KAP3 (KIF3A:KIF3B ∼1; Fig. 3B). Taken together, these data suggest that GLI2 can interact with kinesin-2 motors, and that GLI2 preferentially interacts with KIF3A.

Because the majority of KAP3 in the cell associates with KIF3A–KIF3B (Yamazaki et al., 1995; Yamazaki et al., 1996), we examined whether the co-expression of KAP3A with KIF3A or KIF3B would promote interactions with GLI2. We immunoprecipitated MYC::GLI2 from COS-7 cells expressing KAP3A::FLAG and either KIF3A::HA (Fig. 3C) or KIF3B::HA (Fig. 3D). Strikingly, co-expression of KAP3A and KIF3A resulted in significantly more co-precipitation of both proteins with GLI2 compared to that observed following expression of either protein individually (Fig. 3C; upper panel, cf. lane 5 and lane 8; second panel, cf. lane 6 and lane 8). In stark contrast to this, co-expression of KAP3A and KIF3B did not enhance the amount of KIF3B (Fig. 3D; upper panel, cf. lane 5 and lane 8) or KAP3A (Fig. 3D; second panel, cf. lane 6 and lane 8) that co-precipitated with GLI2. Taken together, these data suggest that GLI2 preferentially interacts with KIF3A rather than KIF3B and that co-expression of KIF3A and KAP3A promotes synergistic interactions of both proteins with GLI2.

The armadillo repeats in KAP3 mediate interactions with GLI2

We next performed a complementary set of biochemical experiments to determine the regions within KAP3A and KIF3A that are required to interact with GLI proteins. Previous work has indicated that KAP3A interacts with cargo proteins through its armadillo repeats (Gindhart and Goldstein, 1996; Jimbo et al., 2002; Morris et al., 2004; Brown et al., 2005); however, whether KAP3A interacts with GLI proteins in a similar manner is unclear. To test this, we generated two epitope-tagged truncated versions of KAP3A (KAP3AΔC::HA and KAP3AΔN::HA; Fig. 3E). These constructs delete >100 amino acids C-terminal (KAP3ΔC) or N-terminal (KAP3ΔN) to the centrally located armadillo repeats of KAP3. Immunoprecipitation of GLI2 co-precipitated full-length KAP3A, KAP3AΔC and KAP3AΔN (Fig. 3F). These data are consistent with the notion that the armadillo repeats in KAP3A mediate interactions with GLI2. Attempts to identify specific armadillo repeats in KAP3 that are required to interact with GLI proteins were hindered by poor expression of these constructs, thus precluding further analysis (data not shown).

The N-terminal motor domain of KIF3A is dispensable for interactions with GLI2

To map the domain within KIF3A that mediates interactions with GLI proteins, we immunoprecipitated MYC::GLI2 from cells expressing either KIF3A::HA or a version of KIF3A that lacks the conserved N-terminal motor domain, DNKIF3A::HA (Fig. 3G). KIF3A and DNKIF3A both co-precipitated with GLI2, albeit less strongly when compared with KAP3A (Fig. 3H, upper panels). Notably, DNKIF3A was expressed at lower levels than full-length KIF3A, which might explain the quantitative difference in GLI2 association (Fig. 3H, lower panels). Regardless, these data indicate that the motor domain of KIF3A is dispensable for interactions with GLI2.

KAP3A interacts with a constitutive GLI repressor, but not a constitutive GLI activator

Given that GLI1–3 interact with KAP3, we sought to identify the domains within the GLI proteins that mediate binding to KAP3. Specifically, we examined the requirements for the N- and C-termini of the GLI proteins in KAP3 interactions (Fig. 4). Here, we took advantage of the high degree of sequence conservation shared between mammalian GLI2 and GLI3 proteins. GLI2 and GLI3 contain a conserved N-terminal transcriptional repressor domain and a carboxy-terminal transcriptional activation domain (Sasaki et al., 1999). We generated two constructs – one that encodes an epitope-tagged, N-terminal-truncated, constitutively active GLI2 (MYC::GLI2ΔN; Roessler et al., 2005; Fig. 4A) and a second that encodes an epitope-tagged, C-terminal-truncated GLI3 (MYC::GLI3R; Fig. 4E) that functions as a constitutive transcriptional repressor (Meyer and Roelink, 2003).

Journal of Cell Science (2015) 128, 1034–1050 doi:10.1242/jcs.162552

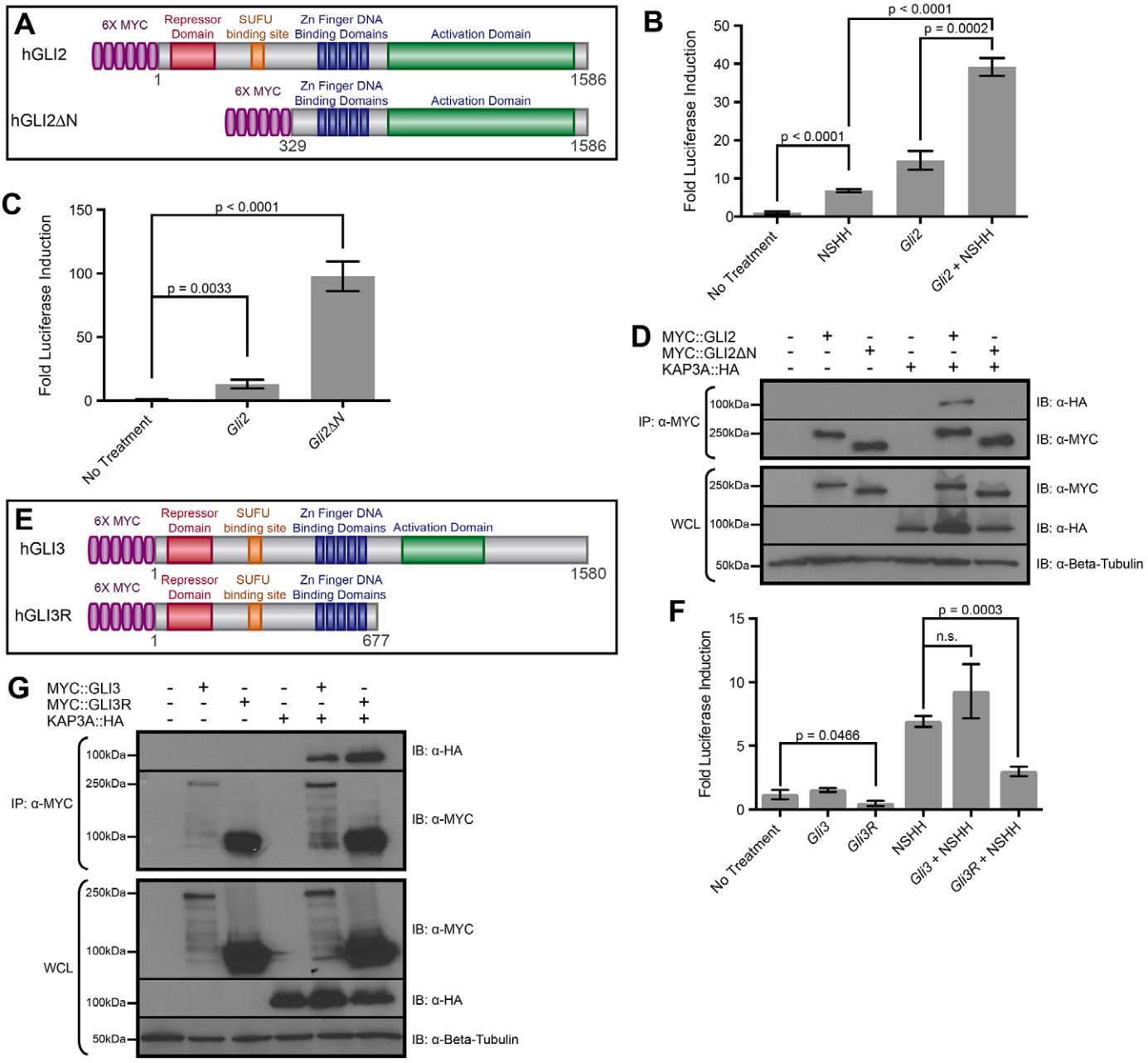

Fig. 4. The N-termini of GLI2 and GLI3 interact with KAP3A. (A) Schematic of full-length and truncated human (h)GLI2 proteins. A 6×MYC epitope tag (purple) is present at the N-terminus of each GLI2 protein. Highly conserved GLI2 protein sequences include a transcriptional repressor domain (red, absent from hGLI2ΔN), SUFU binding site (orange, absent from hGLI2ΔN), five zinc-finger DNA-binding domains (dark blue), a phosphorylation cluster (light blue) and a transcriptional activation domain (green). (B) Luciferase activity readout of HH signaling following treatment of NIH/3T3 fibroblasts with NSHH after transfection with either empty vector (No Treatment) or *Gli2*-pCDNA3 (*Gli2*). HH pathway activity is measured as the fold luciferase induction. Data represent the mean±s.d. for triplicate samples from a single experiment and are representative of three independent experiments; *P*-values are indicated above the relevant treatment groups (Student's unpaired *t*-test). (C) Comparison of HH pathway activity in NIH/3T3 cells expressing hGLI2 or hGLI2ΔN. (D) Immunoprecipitation of MYC-tagged GLI2 (MYC::GLI2) or GLI2ΔN (MYC::GLI2ΔN) from COS-7 cells co-expressing HA-tagged KAP3A (KAP3A::HA). Immunoprecipitates (IP) and whole-cell lysates (WCL) were subjected to SDS-PAGE and western blot analysis (IB) using antibodies directed against MYC (α-MYC) and HA (α-HA). Antibody detection of β-tubulin (α-Beta-Tubulin) was used to confirm equal loading across lanes. The molecular masses (in kDa) of protein standards are indicated at the left of each blot. (E) Schematic of full-length and truncated human GLI3 proteins. (F) Luciferase activity readout of HH signaling following treatment of NIH/3T3 fibroblasts with NSHH after transfection with either empty vector (No Treatment), *Gli3*-pCDNA3 (*Gli3*) or *Gli3R*-pCDNA3 (*Gli3R*). HH pathway activity is measured as the fold luciferase induction. Data represent the mean±s.d. for triplicate samples in a single experiment and are representative of three independent experiments; *P*-values are indicated above the relevant treatment groups (Student's unpaired *t*-test). n.s., not significant ($P>0.05$). (G) Immunoprecipitation of MYC-tagged GLI3 (MYC::GLI3) or GLI3R (MYC::GLI3R) from COS-7 cells co-expressing KAP3A::HA.

To confirm the activity of these constructs, we tested their function in a cell-based HH reporter assay. Consistent with previous reports, full-length GLI2 induced an approximately 12-fold increase in HH-dependent luciferase expression in NIH/3T3 fibroblasts compared with no treatment (Kim et al., 2009; Fig. 4B). This is similar to the level of induction observed when cells are exposed to N-terminal Sonic Hedgehog (NSHH)-conditioned medium (Fig. 4B). Importantly, we observed a synergistic induction of luciferase activity (~40-fold induction) when *Gli2*-transfected cells were also treated with NSHH-conditioned medium (Fig. 4B). These results confirm that MYC::GLI2 functions to activate HH-dependent transcription in NIH/3T3 cells.

In contrast to full-length GLI2, expression of constitutively active MYC::GLI2ΔN resulted in ~90-fold induction of luciferase activity (Fig. 4C). These results support those of previous studies (Roessler et al., 2005; Sasaki et al., 1999) and confirm that MYC::GLI2ΔN functions to activate HH signaling at high levels in mammalian cells. To determine the requirement for the N-terminal domain of GLI2 in mediating KAP3 binding, we performed additional co-immunoprecipitation studies (Fig. 4D). Surprisingly, although full-length GLI2 and GLI2ΔN were expressed at similar levels in cell lysates and were precipitated equivalently, KAP3A only co-precipitated with full-length GLI2 and did not significantly interact with GLI2ΔN (Fig. 4D). These data suggest that the N-terminal domain of GLI2 is required to interact with KAP3 proteins.

We next tested MYC::GLI3R activity in luciferase assays and compared its function to that of full-length MYC::GLI3 (Fig. 4F). Unlike GLI2, full-length GLI3 did not induce significant HH pathway activity in the absence of ligand treatment (Fig. 4F). Furthermore, treatment of cells expressing full-length GLI3 with NSHH-conditioned medium did not significantly induce luciferase activity beyond that observed with NSHH treatment alone (Fig. 4F). These data are consistent with the current paradigm that GLI3 functions mainly as a transcriptional repressor *in vivo* (Wang et al., 2000). By contrast, MYC::GLI3R induced a small but significant decrease in luciferase induction when compared with no treatment in the absence of HH ligand treatment (Fig. 4F). Similarly, MYC::GLI3R significantly decreased NSHH-mediated luciferase induction (Fig. 4F). These data confirm that MYC::GLI3R functions as a transcriptional repressor in cell signaling assays.

We performed immunoprecipitation studies with full-length GLI3 and GLI3R to assess interactions with KAP3A (Fig. 4G). Similar to the results presented in Fig. 2, KAP3A co-precipitates with full-length GLI3. Importantly, KAP3A also co-precipitates with GLI3R (Fig. 4G). These data suggest that the N-terminus of GLI3 is sufficient to mediate physical interactions with KAP3A. Notably, immunofluorescence localization data demonstrate that GLI3R is localized exclusively to the nucleus (supplementary material Fig. S3). Taken together, these results further suggest that there is a common N-terminal domain in GLI2 and GLI3 that promotes interactions with KAP3.

The N-terminus of GLI2 interacts with KAP3A

To more precisely map the domains within the GLI proteins that interact with KAP3A, we generated a series of epitope-tagged N-terminal-truncated versions of GLI2 (Fig. 5A). GLI2ΔN, which failed to appreciably interact with KAP3A (Fig. 4D), lacks the N-terminal 328 amino acids of GLI2 (Roessler et al., 2005). Therefore, we generated MYC::GLI2$^{154–1586}$ to determine whether amino acids 154 to 328 mediate KAP3 binding. Similar to GLI2ΔN, and in contrast to full-length GLI2, immunoprecipitation of MYC::GLI2$^{154–1586}$ failed to co-precipitate KAP3A (Fig. 5B). We employed this strategy iteratively, generating MYC::GLI2$^{61–1586}$ to assess whether amino acids 61 to 153 mediate GLI2 interactions with KAP3A. Importantly, GLI2$^{61–1586}$ did co-precipitate similar amounts of KAP3A as compared to full-length GLI2 (Fig. 5B). These data suggest that GLI2 interacts with KAP3A through an N-terminal motif that lies between amino acids 61 and 153.

To test the functional significance of this interaction, we again utilized luciferase reporter assays in HH-responsive NIH/3T3 cells (Fig. 5C). Whereas expression of full-length GLI2 promoted a small but significant increase in luciferase activity, GLI2$^{154–1586}$ induced an ~70-fold increase in luciferase activity, similar to the induction observed with GLI2ΔN (cf. Fig. 4C and Fig. 5C). By contrast, GLI2$^{61–1586}$ promoted much lower levels of signaling (~12-fold), which is similar to the induction observed with full-length GLI2 (Fig. 5C). These data correlate GLI binding to KAP3 with reduced HH pathway activity.

Having narrowed the KAP3-binding domain in GLI2 to an area of <100 amino acids, we generated two additional constructs to more finely map this interaction. We first generated GLI2$^{108–1586}$; similar to GLI2ΔN, GLI2$^{108–1586}$ did not co-precipitate KAP3A as effectively as full-length GLI2 or GLI2$^{61–1586}$ (Fig. 5D). These data suggest that amino acids 61–108 are necessary to interact with KAP3A. Therefore, we also deleted these amino acids from full-length GLI2 (GLI2$^{\Delta 61–108}$; Fig. 5A). GLI2$^{\Delta 61–108}$ does not effectively co-precipitate KAP3A compared with full-length GLI2 (Fig. 5D), confirming that amino acids 61–108 are essential for GLI2 interactions with KAP3.

To further test the correlation between GLI::KAP3 interactions and reduced HH pathway activity (Fig. 5C), we examined whether deletion of the domain responsible for KAP3 binding might result in higher GLI activity. Indeed, GLI2$^{\Delta 61–108}$ promotes approximately threefold greater luciferase induction than full-length GLI2 in cell signaling assays (Fig. 5E). Taken together, these data identify an interaction between GLI2 and KAP3A that is mediated by 47 amino acids within the N-terminus of GLI2 that acts to restrict GLI2 activity.

KAP3A interactions with GLI3 do not alter GLI repressor function

To test whether the KAP3-binding domain identified in GLI2 could also mediate interactions between GLI3 and KAP3A, we generated a MYC::GLI3R$^{\Delta 134–182}$ construct that contained a deletion of the analogous motif in GLI3 (Fig. 6A). Similar to GLI2$^{\Delta 61–108}$ (Fig. 5D), GLI3R$^{\Delta 134–182}$ did not effectively co-precipitate KAP3A compared with full-length GLI3 and GLI3R (Fig. 6B), demonstrating that the 47-amino-acid KAP3-binding domain is conserved between GLI2 and GLI3.

We also compared the repressor function of GLI3R to GLI3R$^{\Delta 134–182}$ in the presence of NSHH-mediated luciferase induction (Fig. 6C). Surprisingly, and in stark contrast to the transcriptional activation data obtained with GLI2, GLI3R and GLI3R$^{\Delta 134–182}$ were equally effective in repressing HH pathway activation (from ~4.5-fold to 1.5-fold), suggesting that perturbing the interaction between GLI3R and KAP3 does not alter GLI3 repressor activity (Fig. 6C). Taken together, these data indicate that the KAP3-binding domain is conserved between GLI2 and GLI3, and that KAP3 binding selectively restricts GLI activator but not GLI repressor function.

Journal of Cell Science (2015) 128, 1034–1050 doi:10.1242/jcs.162552

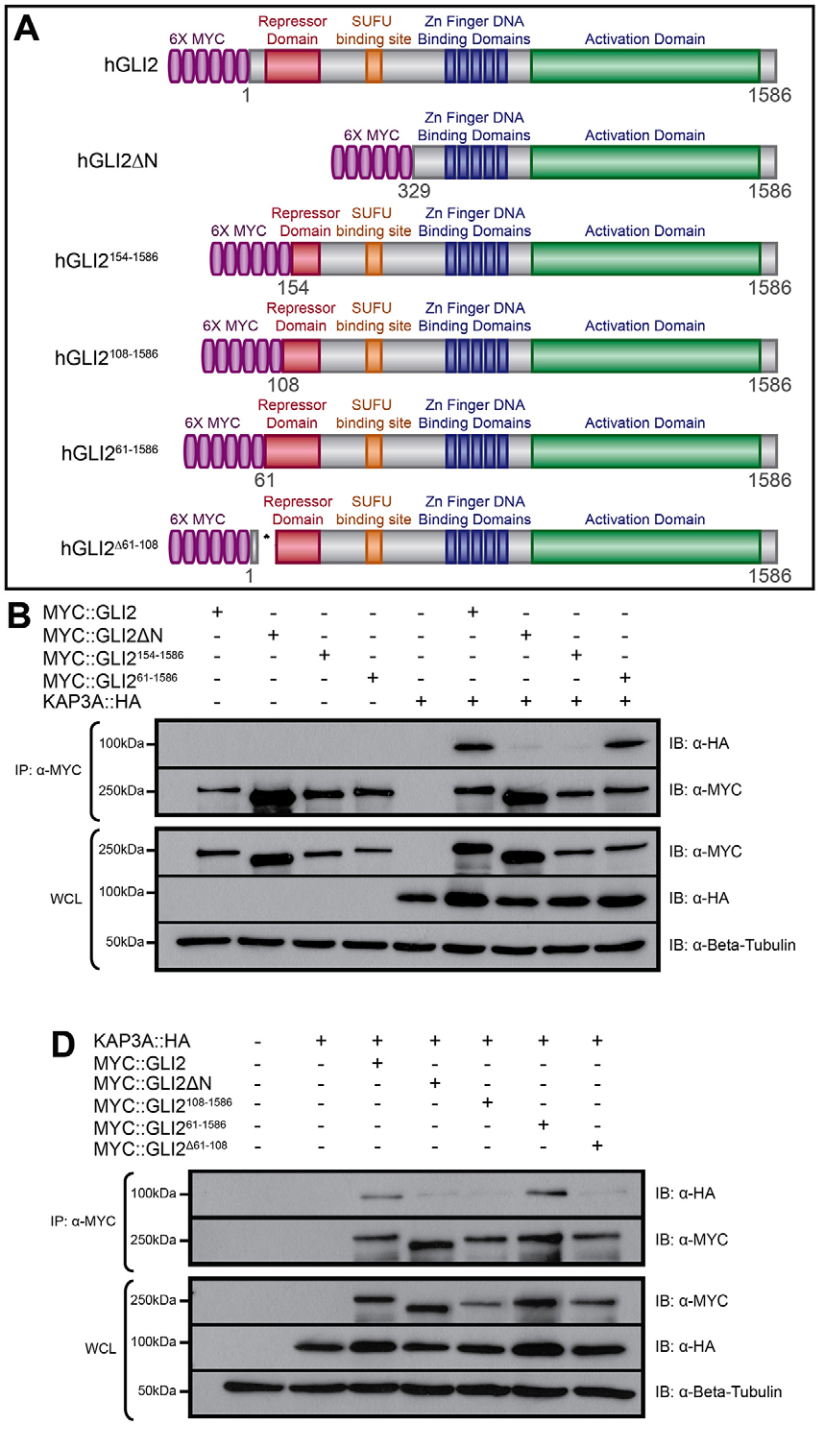

Fig. 5. GLI2 interacts with KAP3A through an N-terminal domain that restricts GLI2 function. (A) Schematic of full-length and truncated human (h)GLI2 proteins. (B) Immunoprecipitation of MYC-tagged GLI2 (MYC::GLI2), GLI2ΔN (MYC::GLI2ΔN), GLI2$^{154–1586}$ (MYC::GLI2$^{154–1586}$) or GLI2$^{61–1586}$ (MYC::GLI2$^{61–1586}$) from COS-7 cells expressing HA-tagged KAP3A (KAP3A::HA). (C) Luciferase activity readout of HH signaling after transfection with either empty vector (No Treatment), *Gli2*, *Gli2*$^{154–1586}$ or *Gli2*$^{61–1586}$. HH pathway activity is measured as the fold luciferase induction. Data represent the mean±s.d. for triplicate samples in a single experiment and are representative of three independent experiments; *P*-values are indicated above the relevant treatment groups (Student's unpaired *t*-test). (D) Immunoprecipitation of MYC::GLI2, MYC::GLI2ΔN, MYC::GLI2$^{108–1586}$, MYC::GLI2$^{61–1586}$ or MYC::GLI2$^{Δ61–108}$ from COS-7 cells expressing KAP3A::HA. Immunoprecipitates (IP) and whole-cell lysates (WCL) were subjected to SDS-PAGE and western blot analysis (IB) using antibodies directed against MYC (α-MYC) and HA (α-HA). Antibody detection of β-tubulin (α-Beta-Tubulin) was used to confirm equal loading across lanes. The molecular masses (in kDa) of protein standards are indicated at the left of each blot. (E) Comparison of full-length GLI2 and GLI2$^{Δ61–108}$ activity in HH-responsive NIH/3T3 cells. Data represent the mean±s.d. for triplicate samples in a single experiment and are representative of three independent experiments; *P*-values are indicated above the relevant treatment groups (Student's unpaired *t*-test).

Journal of Cell Science (2015) 128, 1034–1050 doi:10.1242/jcs.162552

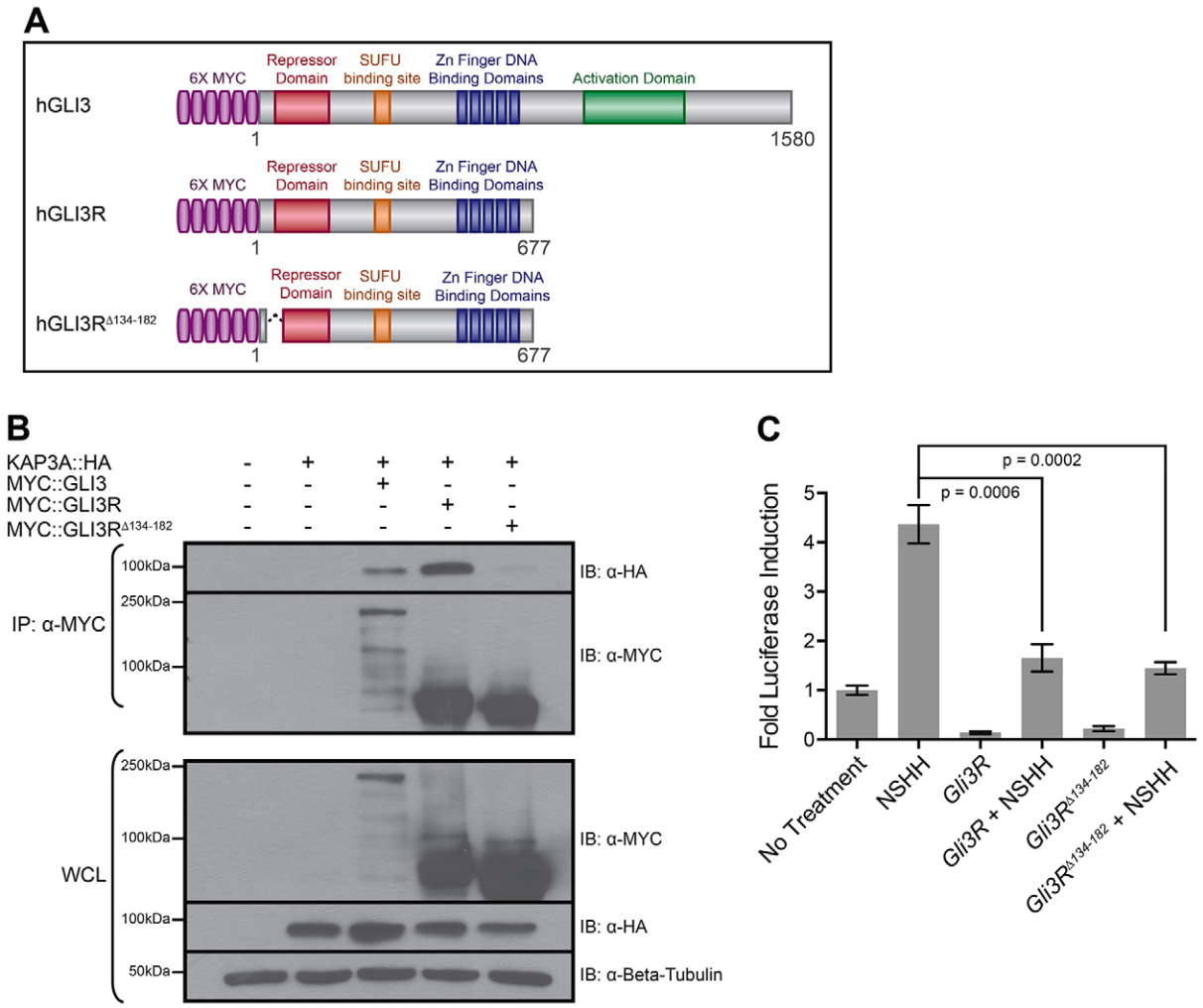

Fig. 6. KAP3A interacts with an N-terminal GLI3 domain that does not alter GLI repressor function. (A) Schematic of full-length and truncated human (h)GLI3 proteins. (B) Immunoprecipitation (IP) of MYC-tagged GLI3 (MYC::GLI3), GLI3R (MYC::GLI3R) or GLI3R$^{\Delta 134–182}$ (MYC::GLI3R$^{\Delta 134–182}$) from COS-7 cells expressing HA-tagged KAP3A (KAP3A::HA). Immunoprecipitates (IP) and whole-cell lysates (WCL) were subjected to SDS-PAGE and western blot analysis (IB) using antibodies directed against MYC (α-MYC) and HA (α-HA). Antibody detection of β-tubulin (α-Beta-Tubulin) was used to confirm equal loading across lanes. (C) Luciferase activity readout of HH signaling after transfection with empty vector (No Treatment), *Gli3R* or *Gli3*$^{\Delta 134–182}$. HH pathway activity is measured as the fold luciferase induction. Data represent the mean±s.d. for triplicate samples in a single experiment and are representative of three independent experiments; *P*-values are indicated above the relevant treatment groups (Student's unpaired *t*-test).

KAP3 interactions with GLI2 restrict HH pathway activation *in vivo*

To extend the observation that KAP3–GLI interactions selectively restrict GLI activator but not GLI repressor function, we utilized chicken *in ovo* neural tube electroporation (Fig. 7). Here, we can assess the consequences of GLI function on the expression of endogenous HH targets to read out different levels of HH pathway activation, including those targets (e.g. NKX2.2) that exclusively require GLI activator function for their expression (Bai et al., 2004; Bai and Joyner, 2001; Bai et al., 2002; Oosterveen et al., 2012; Peterson et al., 2012).

Electroporation of empty vector (*pCIG*) did not alter expression of the low-level HH pathway target, NKX6.1 (Fig. 7A). By contrast, electroporation of *Gli2* promoted cell autonomous ectopic NKX6.1 expression, as did electroporation of a KAP-binding-deficient *Gli2* construct (*Gli2*$^{\Delta 61–108}$) and constitutively active *Gli2ΔN* (Fig. 7A). Strikingly, GLI2 was not sufficient to promote ectopic NKX2.2 expression in the developing neural tube, whereas expression of a KAP3-binding-deficient GLI2 (GLI2Δ61–108) did induce cell-autonomous NKX2.2 expression, similar to what was observed with expression of constitutively active GLI2ΔN (Fig. 7B). Notably, ectopic NKX2.2+ cells were detected even in the dorsal-most aspect of the chicken neural tube (Fig. 7B, arrows).

To test whether KAP3-binding-deficient GLI3R (GLI3RΔ134–182) is sufficient to repress endogenous HH target genes in the developing chicken neural tube, we electroporated GLI3R and GLI3RΔ134–182 and assessed PAX7 expression (supplementary material Fig. S4). Whereas HH signaling normally restricts PAX7 expression to the dorsal neural tube, electroporation of GLI3R resulted in ventral expansion of PAX7 even in the ventral-most aspect of the neural tube (supplementary material Fig. S4A, upper row, white arrows). Similar to GLI3R, the KAP3-binding-deficient GLI3R (GLI3RΔ134–182) induced ectopic PAX7

Journal of Cell Science (2015) 128, 1034–1050 doi:10.1242/jcs.162552

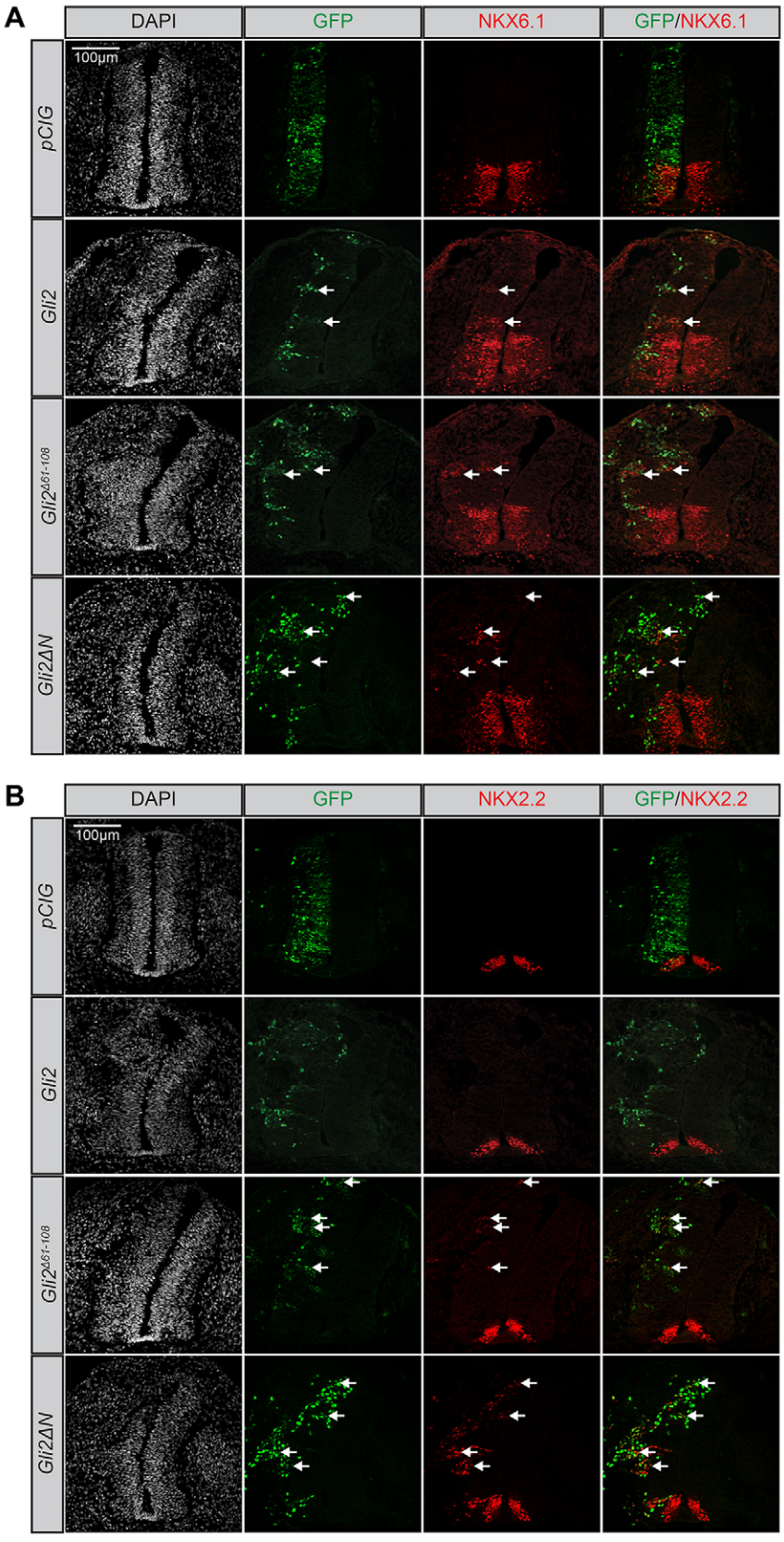

Fig. 7. KAP3 binding restricts GLI2 activity *in vivo*. (A) Transverse sections of Hamburger-Hamilton stage 21–22 chicken neural tubes electroporated with *pCIG* (upper row), *Gli2* (upper middle row), *Gli2*$^{\Delta 61-108}$ (lower middle row) or *Gli2ΔN* (lower row) were stained with antibodies raised against NKX6.1 (red). GFP-expressing cells (green) denote electroporated cells. DAPI marks nuclei. Arrows indicate ectopic expression of NKX6.1. (B) Transverse sections of Hamburger-Hamilton stage 21–22 chicken neural tubes stained with antibodies raised against NKX2.2 (red). GFP-expressing cells (green) denote electroporated cells. DAPI marks nuclei. Arrows indicate ectopic NKX2.2 expression.

expression throughout the ventral neural tube (supplementary material Fig. S4A, lower row, white arrows). Taken together, these data support the notion that KAP3-binding restricts the activator but not repressor function of the GLI proteins.

DISCUSSION

GLI proteins physically interact with the heterotrimeric kinesin-2 motor complex

Tightly regulated trafficking and processing of GLI proteins are vital for proper HH signaling (Haycraft et al., 2005; Kim et al., 2009). However, the mechanisms that regulate GLI protein function remain poorly understood. Here, we present evidence that the heterotrimeric KIF3A–KIF3B–KAP3 kinesin-2 motor complex selectively regulates GLI activator function through multiple physical interactions (Fig. 8A). Specifically, we find that all three mammalian GLI proteins physically interact with the kinesin-associated protein, KAP3. Furthermore, we demonstrate that GLI2 and GLI3 interact with KAP3 through a conserved N-terminal 47-amino-acid domain that restricts GLI activator but not GLI repressor function. We also map the GLI-binding site in KAP3 to the conserved armadillo repeats that mediate interactions with other KAP3 cargo proteins (Gindhart and Goldstein, 1996; Jimbo et al., 2002; Phang et al., 2014). In addition, we find that GLI proteins selectively interact with the KIF3A kinesin-2 motor component, but not appreciably with KIF3B. Strikingly, GLI proteins interact synergistically with KIF3A and KAP3, forming a robust complex that suggests GLI protein function is regulated by multiple interactions with the kinesin-2 motor complex. To our knowledge, this study provides the first evidence that GLI proteins physically interact with plus-end-directed kinesin-2 motor proteins, despite their implication in HH signaling for over a decade (Takeda et al., 1999; Huangfu et al., 2003). These results are of particular significance given that ciliary transport of cargo is currently believed to be largely mediated by interactions with IFT particles (Scholey, 2003; Bhogaraju et al., 2013; Qin et al., 2004). However, our data suggest a novel paradigm where direct interactions of kinesin-2 motors with GLI protein cargo can regulate their trafficking and function. Notably, these results are consistent with recent work suggesting that kinesin-2 motors also mediate the anterograde trafficking of dynein proteins independently of IFT particles (Hao et al., 2011). Further studies are needed to elucidate whether ciliary trafficking of GLI proteins occurs independently of IFT and BBSome protein interactions.

Complex regulation of GLI protein processing and activity

Multiple proteins modulate GLI transcriptional activity to control the output of HH signaling. Suppressor of Fused (SUFU) represses HH signaling by binding to GLI proteins and preventing their nuclear transport (Kogerman et al., 1999; Barnfield et al., 2005). SUFU–GLI complexes traffic to primary cilia in response to HH stimulation, a process necessary for dissociation of the complex and subsequent nuclear translocation of GLI proteins (Tukachinsky et al., 2010), but the mechanisms that control complex assembly and/or disassembly are unclear. Here, we show that KAP3 interacts with GLI2 and GLI3 and colocalizes with these proteins in primary cilia. KAP3 might control GLI activity through effects on SUFU–GLI complex formation. However, interactions between KAP3 and the constitutively nuclear-localized GLI3R also suggest a role for KAP3 at the level of nuclear trafficking. It is plausible that the KIF3A–KIF3B–KAP3 complex controls both the nuclear and ciliary trafficking of GLI proteins, but further experiments are required to elucidate these mechanisms. It will be of particular interest to test whether KAP3 affects SUFU–GLI interactions and the requirement for cilia in this process.

KAP3 interactions with GLI proteins specifically regulate GLI activator function

We demonstrate that a conserved 47-amino-acid domain in GLI2 and GLI3 mediates KAP3 interactions, and that deletion of this domain from GLI2 results in increased transcriptional activity. Notably, this motif encompasses a portion of a previously identified N-terminal repressor domain (Sasaki et al., 1999). As a result, one possibility is that the increase in GLI2 activity is simply due to loss of this poorly defined repressor domain. However, two key findings argue against this notion. First, elimination of the analogous domain in GLI3 does not alter GLI3 repressor function, suggesting that this domain does not possess general repressive activity. Second, electroporation of a KAP-binding-deficient *Gli2* construct in the developing chicken neural tube induces ectopic NKX2.2 expression, which requires GLI activator function and cannot be induced simply by the loss of GLI repression (Matise et al., 1998; Bai et al., 2004). Taken together, these data support a novel paradigm where GLI–KAP3 interactions selectively restrict the activator but not the repressor function of GLI proteins.

These observations are similar to SUFU regulation of GLI proteins, where GLI3 repressor can function independently of SUFU (Wang et al., 2010). In these studies, SUFU interacts with both GLI2 and GLI3; however, GLI3 repressor is able to rescue the ventralized neural tube phenotype in $Sufu^{-/-}$ embryos (Wang et al., 2010). It is interesting to speculate that, similar to SUFU, KAP3 might regulate GLI activator proteins during transit to the nucleus, although the nature of GLI, KAP3 and SUFU interplay will require further study.

Regulation of GLI function by kinesin proteins

Initial studies in *Drosophila* identified Cos2 (also known as Cos) as a kinesin-related protein that controls HH signaling through interactions with Ci, the *Drosophila* homolog of GLI (Sisson et al., 1997; Robbins et al., 1997). More recent studies in vertebrates identified a similar role for the *Cos2* homolog, *Kif7*, in the regulation of GLI protein function (Liem et al., 2009; Endoh-Yamagami et al., 2009; Cheung et al., 2009). In particular, KIF7, and the structurally related kinesin KIF27, both interact with GLI proteins (Endoh-Yamagami et al., 2009; Cheung et al., 2009; Maurya et al., 2013; Marks and Kalderon, 2011), whereas KIF7 specifically functions to both promote and antagonize GLI activity (Maurya et al., 2013; Hsu et al., 2011; Li et al., 2012). KIF7 promotes HH signaling through dissociation of SUFU–GLI complexes, and controls the ciliary localization of GLI proteins in a tissue-specific manner (Hsu et al., 2011; Maurya et al., 2013; Endoh-Yamagami et al., 2009). Although the KIF7–GLI interaction sites have not been precisely mapped, GLI proteins appear to interact with KIF7 through multiple domains, including an N-terminal motif (Marks and Kalderon, 2011). One hypothesis is that KAP3 competes for KIF7 binding to GLI proteins, thus limiting the dissociation of GLI–SUFU complexes and restricting GLI protein function. Interestingly, KIF7 functions to organize the ciliary tip compartment through the regulation of microtubule dynamics (He et al., 2014). Furthermore, the effects of KIF7 are controlled by PPFIA1- and PP2A-mediated regulation of KIF7 phosphorylation (Liu et al., 2014). These results suggest that either the loss of KIF7 (He et al., 2014) or altered KIF7

Journal of Cell Science (2015) 128, 1034–1050 doi:10.1242/jcs.162552

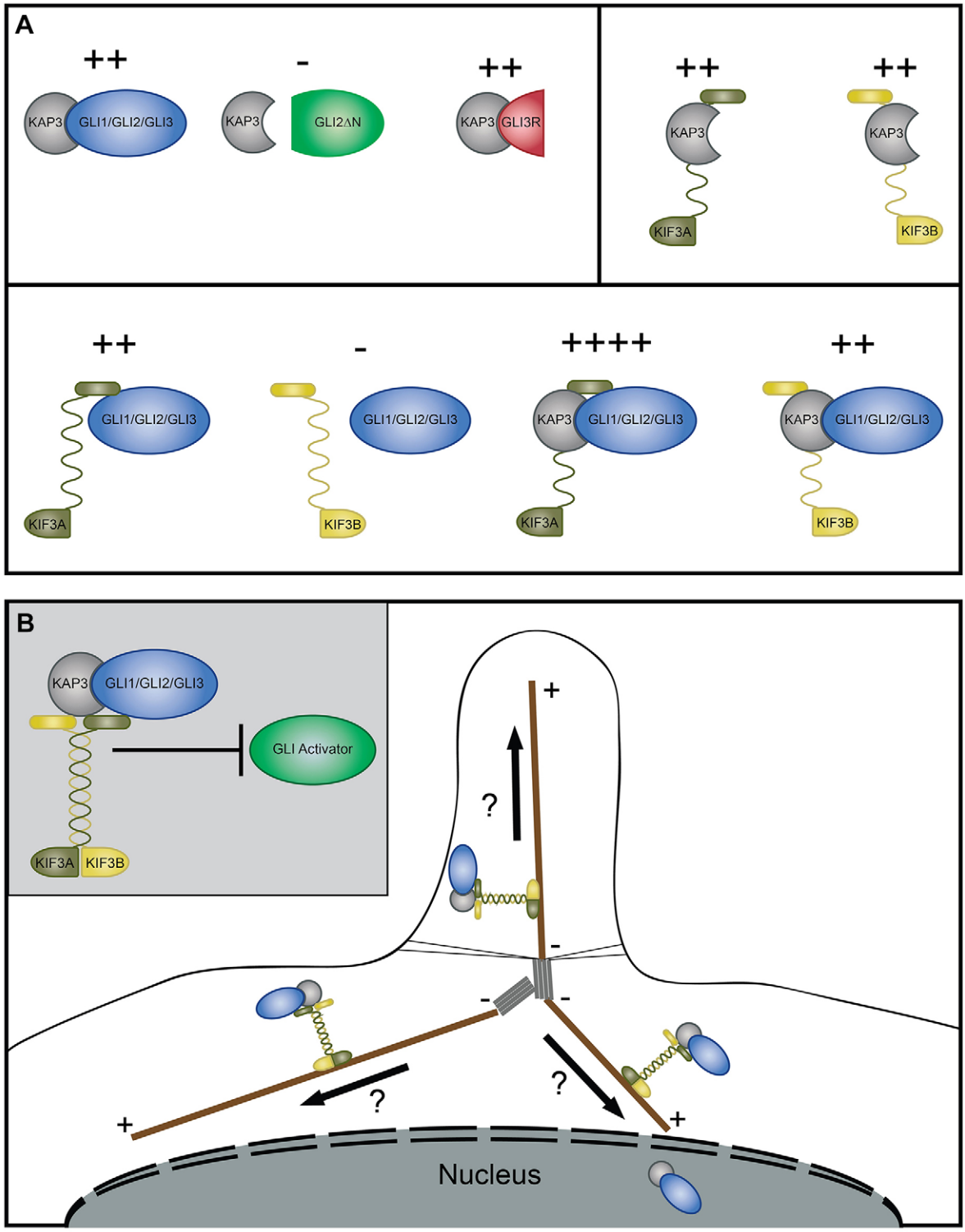

Fig. 8. Model of GLI–kinesin-2 complex interactions and subcellular localization. (A) Schematic summary of biochemical interactions between GLI proteins (blue), KAP3 (gray), KIF3A (dark green) and KIF3B (yellow). Truncated versions of GLI proteins, GLI2ΔN and GLI3R, are represented in light green and red, respectively. Plus (+) and minus (−) represent the relative strength of interaction based on the immunoprecipitation studies, with − indicating no interaction and ++++ denoting the strongest interaction. (B) Schematic of the functional consequence of the KAP3–GLI interaction on GLI activator (green) and subcellular localization of the GLI (blue)–KAP3 (gray)–KIF3A (dark green)–KIF3B (yellow) complex. The primary cilium is represented by microtubules (brown) extending from basal bodies (gray) with the ciliary barrier depicted by thin black lines. Plus (+) and minus (−) depict microtubule directionality. Question marks denote putative plus-end trafficking roles for KIF3A–KIF3B–KAP3 in regulating GLI proteins based on biochemical, immunofluorescence and signaling studies.

Journal of Cell Science (2015) 128, 1034–1050 doi:10.1242/jcs.162552

phosphorylation (Liu et al., 2014) affects the ciliary localization and activity of GLI proteins. However, given that KIF7 does not possess plus-end-directed microtubule motor activity (He et al., 2014), one possibility is that KAP3–GLI protein interactions are disrupted in *Kif7*-mutant cells owing to the disorganized ciliary tip compartments. It will be particularly important to test these interactions in cells with different KIF7 expression levels and phosphorylation states, and to assess the role of KIF7 in mediating kinesin-2 interactions with GLI proteins.

Our data indicate that, in addition to KIF7 and KIF27, GLI proteins also interact with KIF3A, suggesting that multiple kinesin proteins control GLI function. That KIF3A interacts with GLI proteins independently of KAP3 has precedent in the literature. For example, the TRIM protein RNF33 (also known as TRIM60) interacts with KIF3A and KIF3B in mouse testis (Huang et al., 2012). Additionally, the protein phosphatases DUSP26 and POPX2 (also known as PPM1F) interact with both KIF3 and KAP3 proteins (Tanuma et al., 2009; Phang et al., 2014). These data also raise the question of whether GLI proteins interact with yet additional kinesin proteins. Our results indicate that GLI2 preferentially interacts with KIF3A but not KIF3B, analogous to earlier data demonstrating selective interactions of GLI2 with KIF7 and KIF27 (Cheung et al., 2009). Future studies will be required to determine whether GLI proteins interact with: (1) additional kinesin-2 motors, including KIF3C and KIF17 (Yang et al., 2001; Yang and Goldstein, 1998; Insinna et al., 2008; Snow et al., 2004), (2) other kinesin motors implicated in ciliary trafficking (Morsci and Barr, 2011) and (3) non-ciliary kinesin motors (Hirokawa et al., 2009).

In addition to kinesin-2 motors and their adaptor proteins, IFT particles, such as IFT25 and IFT122, also regulate GLI ciliary localization (Qin et al., 2011; Keady et al., 2012). However, whether this is mediated by physical interactions between GLI and IFT particles remains unexplored, and whether KAP3 interacts directly with these IFT particles has not been tested. One possibility is that, along with KAP3, IFT particles interact with GLI proteins to mediate ciliary GLI trafficking. In addition to their role in ciliary trafficking, IFT particles also function in trafficking outside of the primary cilium (reviewed by Baldari and Rosenbaum, 2010). For example, IFT particles traffic T-cell receptors to the immune synapse (Finetti et al., 2009). Future studies will determine whether IFT particles interact with GLI proteins and the consequences of these interactions on GLI processing and activity.

In summary, despite the indirect role of KIF3A–KIF3B–KAP3 in HH signaling owing to their role in ciliogenesis, the issue of whether these motors control HH signaling directly through interactions with HH pathway components has remained unexplored. Here, we identify GLI proteins as novel cargo of the heterotrimeric kinesin-2 motor complex that physically interact with KAP3 and selectively interact with KIF3A but not KIF3B. Based on our data, we propose a model (Fig. 8B) where GLI proteins interact with kinesin-2 motors through synergistic interactions with KAP3 and KIF3A that selectively restrict GLI activator but not GLI repressor function. We postulate that kinesin-2 motors might regulate: (1) anterograde GLI trafficking to ciliary tips, (2) GLI trafficking to the nucleus following ciliary transport or (3) GLI transport to other cellular compartments (Fig. 8B). Although the precise molecular mechanism awaits elucidation, our findings identify a direct role for the kinesin-2 motor protein complex in HH signaling through physical interactions with GLI proteins that selectively regulate GLI transcriptional activity.

MATERIALS AND METHODS

DNA constructs

To generate 6×MYC-tagged constructs, murine (m)*Gli1*, human (h)*Gli2*, h*Gli2ΔN*, h$Gli2^{280–1586}$, h$Gli2^{262–1586}$, h$Gli2^{218–1586}$, h$Gli2^{154–1586}$, h$Gli2^{108–1586}$, h$Gli2^{61–1586}$, h*Gli3* and h*Gli3R* cDNAs were cloned into pCDNA3 using standard molecular biology techniques. To generate a version of hGLI2 lacking amino acids 61–108 (h$Gli2Δ^{61–108}$), we amplified h*Gli2* using forward (5′-TCTTGCCACCATTCCATGCG-GCTGGCCCTGGGGAGTCCCC-3′) and reverse (5′-GGGGACTC-CCCAGGGCCAGCCGCATGGAATGGTGGCAAGA-3′) mutagenesis primers. To generate a version of hGLI3R lacking amino acids 134–182 (h$GLI3R^{Δ134–182}$) we amplified h*GLI3R* using forward (5′-TTTTC-CCTGCCTTCCATCCTACTGCTGCTTCCGAGTCTCC-3′) and reverse (5′-GGAGACTCGGAAGCAGCAGTAGGATGGAAGGCAGGGAAAA-3′) mutagenesis primers. Hemagglutinin (HA)-tagged h*Kap3a*, h*Kap3b*, h*Kif3a*, h*DNkif3a* and m*Kif3b*, FLAG-tagged h*Kap3a*, HA-tagged h*Gli2ΔN* and 6×MYC-tagged h*Gli2* and h$Gli2^{Δ61–108}$ cDNAs were cloned into pCIG (Megason and McMahon, 2002). *Gli* cDNAs were provided by Drs Bradley Yoder (University of Alabama) and Andrzej Dlugosz (University of Michigan). *Zic1* cDNA was supplied by Dr Kate Barald (University of Michigan).

Immunoprecipitation and western blot analysis

COS-7 cells were transiently transfected with the relevant DNA constructs using Lipofectamine 2000 (Invitrogen, catalog number 11668). The cells were lysed 48 h after transfection in HEPES lysis buffer (25 mM HEPES pH 7.4, 115 mM KOAc, 5 mM NaOAc, 5 mM $MgCl_2$, 0.5 mM EGTA and 1% Triton X-100) containing protease inhibitor (Roche, catalog number 11836153001). Cell lysates were then subjected to centrifugation at 14,000 ***g*** for 15 min to remove the insoluble fraction, and protein concentrations were determined using a bicinchoninic acid (BCA) Assay Kit (Pierce, catalog number 23225). Cell lysates (1 mg) were then pre-cleared with Protein-G–agarose beads (Roche, catalog number 11719416001) for 1 h at 4℃. MYC- or HA-tagged proteins were immunoprecipitated from pre-cleared lysates using either anti-MYC (1:150; Santa Cruz, sc-40) or anti-HA (1:300; Covance, MMS-101) antibodies for 2 h at 4℃. Following immunoprecipitation, the lysates were incubated with Protein-G–agarose beads for 1 h at 4℃. The Protein-G–agarose beads were subjected to five 8-min washes in HEPES lysis buffer and resuspended in 30 µl of 1× PBS and 6× Laemmli buffer. The samples were boiled for 10 min and proteins were separated using SDS-PAGE and analyzed by western blotting. Anti-MYC (1:1000) and anti-HA (1:1000) primary antibodies, peroxidase-conjugated AffiniPure goat anti-mouse-light-chain secondary antibody (1:50,000, Jackson ImmunoResearch, 115-035-174) and a Konica Minolta SRX-101A medical film processor were used to visualize tagged proteins. Western blots were quantified using ImageJ software.

Purification and immunoprecipitation of FLAG-tagged proteins

For purification of GFP::FLAG, KAP3A::FLAG and FLAG::GLI1, COS-7 cells were transfected with the appropriate DNA expression constructs. At 48 h post-transfection, cells were harvested by lysis in a solution containing 50 mM HEPES pH 7.5, 150 mM NaCl, 1% Triton X-100 and a protease inhibitor cocktail. Lysates were centrifuged at 16,000 ***g*** for 15 min. The resulting supernatant was mixed with anti-FLAG M2 agarose beads (Sigma-Aldrich) and incubated for 2 h at 4℃. After extensive washes in lysis buffer, bound proteins were eluted from the beads with two 20-min incubations with 300 µg/ml of 3× FLAG peptide (ApexBio) at 25℃. Post-elution lysates were subjected to SDS-PAGE and analyzed by Gel Code Blue staining (Thermo Scientific). Equal amounts of the eluted FLAG-tagged proteins were combined, and KAP3A::FLAG was immunoprecipitated from lysates using mouse anti-KAP3 (BD Biosciences) and the same immunoprecipitation methods described above. A mouse anti-FLAG antibody (1:1000, Sigma-Aldrich), peroxidase-conjugated AffiniPure goat anti-mouse-light-chain secondary antibody (1:50,000, Jackson ImmunoResearch) and a Konica Minolta SRX-101A medical film processor were used to visualize tagged proteins.

Cell culture and luciferase assays

NIH/3T3 cells were cultured at 37℃, 5% CO_2, 95% humidity in Dulbecco's modified Eagle medium (DMEM; Gibco, catalog number 11965-092), containing 10% bovine calf serum (ATCC; catalog number 30-2030) and penicillin-streptomycin-glutamine (Gibco, catalog number 10378-016). Luciferase assays were performed by plating 2.5×10^4 cells/well in 24-well plates. The next day, cells were co-transfected using Lipofectamine 2000 with the DNA constructs indicated in each experiment, in addition to *Ptc*Δ136-GL3 (Chen et al., 1999; Nybakken et al., 2005) and pSV-beta-galactosidase (Promega) constructs to report HH pathway activation and normalize transfections, respectively. Cells were changed to low-serum medium (DMEM supplemented with 0.5% bovine calf serum and penicillin-streptomycin-glutamine) 48 h after transfection and were cultured at 37℃ in 5% CO_2 for an additional 48 h. NSHH-conditioned medium was added immediately after low-serum change where relevant to activate the HH pathway. Cells were harvested, and luciferase and β-galactosidase activities were measured using the Luciferase Assay System (Promega, catalog number E1501) and BetaFluor β-gal assay kit (Novagen, catalog number 70979-3), respectively. Multiple assays were performed and each sample was assayed in triplicate.

Immunofluorescence staining

NIH/3T3 fibroblasts were seeded at a density of 1.5×10^5 cells/well in six-well plates. Cells were transfected 24 h later with either empty vector (pCIG) or with a DNA construct encoding KAP3::HA using Lipofectamine 2000. Cells were grown in low-serum medium starting from 8 h after transfection, fixed 48 h post-transfection in 4% paraformaldehyde (PFA) for 10 min at room temperature and permeabilized with a 5-min incubation in 0.2% Triton X-100 in PBS. Immunostaining was performed using the following primary antibodies: mouse anti-acetylated tubulin (1:2500, Sigma), rabbit anti-γ-tubulin (1:2500, Sigma), mouse anti-KAP3 (1:500, BD Biosciences), rabbit anti-ARL13B (1:500, Proteintech), mouse anti-HA (1:1000, Covance), guinea pig anti-GLI2 (1:300, a gift from Dr Jonathan T. Eggenschwiler, University of Georgia) and mouse anti-GLI3 (1:1000, obtained from Dr Suzie J. Scales, Genentech). The following secondary antibodies were used at a dilution of 1:500: Alexa Fluor 488-conjugated goat anti-guinea-pig IgG, Alexa Fluor 488-conjugated goat anti mouse IgG2b, Alexa Fluor 555-conjugated goat anti-mouse-IgG1 and Alexa Fluor 633-conjugated goat anti-rabbit-IgG. To visualize nuclei, cells were incubated with DAPI (Invitrogen) for 5 min at a dilution of 1:30,000. Cells were imaged using a Leica Upright SP5X White Light Laser Confocal Microscope. Images were processed using Adobe Photoshop and Illustrator.

Chick *in ovo* neural tube electroporation and immunostaining

Electroporation was performed as described previously (Allen et al., 2011). Briefly, DNA (1.0 µg/µl) was injected into the neural tubes of Hamburger-Hamilton stage 10–12 chicken embryos with 50 ng/µl Fast Green. Embryos were dissected after 48 h and fixed in 4% PFA for immunofluorescence analysis. The following antibodies were used for neural tube immunostaining: mouse IgG1 anti-NKX6.1 [1:20, Developmental Studies Hybridoma Bank (DSHB)], mouse IgG1 anti-PAX7 (1:20, DSHB) and mouse IgG2b anti-NKX2.2 (1:20, DSHB). Nuclei were visualized using DAPI (1:30,000, Molecular Probes). Alexa-Fluor-555-conjugated secondary antibodies (1:500, Molecular Probes) were visualized on a Leica Upright SP5X Light Laser Confocal Microscope. Images were processed using Adobe Photoshop and Illustrator.

Acknowledgements

We thank Drs Suzie Scales (Genentech) and Jonathan Eggenschwiler (University of Georgia) for sharing anti-GLI3 and anti-GLI2 antibodies, respectively. We are grateful to Drs Bradley Yoder (University of Alabama-Birmingham) and Andrzej Dlugosz (University of Michigan) for the full-length *Gli* constructs. We also thank Dr Kate Barald (University of Michigan) for providing the *Zic1* construct. We are especially grateful to Dr Bill Tsai and members of his laboratory for critical technical assistance. We thank members of the Allen laboratory for insightful comments and helpful suggestions. The NKX2.2 and NKX6.1 antibodies were obtained from the Developmental Studies Hybridoma Bank developed under the auspices of the National Institute of Child Health and Human Development (NICHD) and maintained by The University of Iowa, Department of Biological Sciences, Iowa City, IA. Confocal microscopy was performed in the Microscopy and Image Analysis Laboratory at the University of Michigan.

Competing interests

The authors declare no competing or financial interests.

Author contributions

B.S.C. and B.L.A. conceived of and designed the experiments. B.S.C. executed the experiments and collected the data. R.L.B. assisted in executing the immunoprecipitation experiments involving KAP3B. B.S.C. and B.L.A. analyzed and interpreted the data. K.J.V. provided kinesin-2 and KAP3 constructs, as well as technical advice, experimental suggestions and help with manuscript preparation and editing. B.S.C. and B.L.A. wrote and edited the manuscript.

Funding

This work was supported by The University of Michigan Center for Organogenesis; an American Heart Association scientist development grant [grant number 11SDG6380000]; and by National Institutes of Health grants [grant numbers R21 CA167122 and R01 DC014428] to B.L.A. and K.J.V. [grant number R01 GM070862]. Deposited in PMC for release after 12 months.

Supplementary material

Supplementary material available online at
http://jcs.biologists.org/lookup/suppl/doi:10.1242/jcs.162552/-/DC1

References

Allen, B. L., Song, J. Y., Izzi, L., Althaus, I. W., Kang, J.-S., Charron, F., Krauss, R. S. and McMahon, A. P. (2011). Overlapping roles and collective requirement for the coreceptors GAS1, CDO, and BOC in SHH pathway function. *Dev. Cell* **20**, 775-787.

Altaba, A. R. I. (1999). Gli proteins encode context-dependent positive and negative functions: implications for development and disease. *Development* **126**, 3205-3216.

Aza-Blanc, P., Lin, H. Y., Ruiz i Altaba, A. and Kornberg, T. B. (2000). Expression of the vertebrate Gli proteins in Drosophila reveals a distribution of activator and repressor activities. *Development* **127**, 4293-4301.

Bai, C. B. and Joyner, A. L. (2001). Gli1 can rescue the in vivo function of Gli2. *Development* **128**, 5161-5172.

Bai, C. B., Auerbach, W., Lee, J. S., Stephen, D. and Joyner, A. L. (2002). Gli2, but not Gli1, is required for initial Shh signaling and ectopic activation of the Shh pathway. *Development* **129**, 4753-4761.

Bai, C. B., Stephen, D. and Joyner, A. L. (2004). All mouse ventral spinal cord patterning by hedgehog is Gli dependent and involves an activator function of Gli3. *Dev. Cell* **6**, 103-115.

Baldari, C. T. and Rosenbaum, J. (2010). Intraflagellar transport: it's not just for cilia anymore. *Curr. Opin. Cell Biol.* **22**, 75-80.

Barnfield, P. C., Zhang, X., Thanabalasingham, V., Yoshida, M. and Hui, C.-C. (2005). Negative regulation of Gli1 and Gli2 activator function by Suppressor of fused through multiple mechanisms. *Differentiation* **73**, 397-405.

Bhogaraju, S., Engel, B. D. and Lorentzen, E. (2013). Intraflagellar transport complex structure and cargo interactions. *Cilia.* **2**, 10.

Briscoe, J. and Thérond, P. P. (2013). The mechanisms of Hedgehog signalling and its roles in development and disease. *Nat. Rev. Mol. Cell Biol.* **14**, 416-429.

Brown, C. L., Maier, K. C., Stauber, T., Ginkel, L. M., Wordeman, L., Vernos, I. and Schroer, T. A. (2005). Kinesin-2 is a motor for late endosomes and lysosomes. *Traffic* **6**, 1114-1124.

Chen, C. H., von Kessler, D. P., Park, W., Wang, B., Ma, Y. and Beachy, P. A. (1999). Nuclear trafficking of Cubitus interruptus in the transcriptional regulation of Hedgehog target gene expression. *Cell* **98**, 305-316.

Cheung, H. O.-L., Zhang, X., Ribeiro, A., Mo, R., Makino, S., Puviindran, V., Law, K. K. L., Briscoe, J. and Hui, C.-C. (2009). The kinesin protein Kif7 is a critical regulator of Gli transcription factors in mammalian hedgehog signaling. *Sci. Signal.* **2**, ra29.

Cole, D. G., Chinn, S. W., Wedaman, K. P., Hall, K., Vuong, T. and Scholey, J. M. (1993). Novel heterotrimeric kinesin-related protein purified from sea urchin eggs. *Nature* **366**, 268-270.

Ding, Q., Motoyama, J., Gasca, S., Mo, R., Sasaki, H., Rossant, J. and Hui, C. C. (1998). Diminished Sonic hedgehog signaling and lack of floor plate differentiation in Gli2 mutant mice. *Development* **125**, 2533-2543.

Endoh-Yamagami, S., Evangelista, M., Wilson, D., Wen, X., Theunissen, J.-W., Phamluong, K., Davis, M., Scales, S. J., Solloway, M. J., de Sauvage, F. J. et al. (2009). The mammalian Cos2 homolog Kif7 plays an essential role in modulating Hh signal transduction during development. *Curr. Biol.* **19**, 1320-1326.

Finetti, F., Paccani, S. R., Riparbelli, M. G. and Giacomello, E. (2009). Intraflagellar transport is required for polarized recycling of the TCR/CD3 complex to the immune synapse. *Nat. Cell Biol.* **11**, 1332-1339.

Gindhart, J. G., Jr and Goldstein, L. S. (1996). Armadillo repeats in the SpKAP115 subunit of kinesin-II. *Trends Cell Biol.* **6**, 415-416.
Goetz, S. C. and Anderson, K. V. (2010). The primary cilium: a signalling centre during vertebrate development. *Nat. Rev. Genet.* **11**, 331-344.
Hao, L., Efimenko, E., Swoboda, P. and Scholey, J. M. (2011). The retrograde IFT machinery of C. elegans cilia: two IFT dynein complexes? *PLoS ONE* **6**, e20995.
Haycraft, C. J., Banizs, B., Aydin-Son, Y., Zhang, Q., Michaud, E. J. and Yoder, B. K. (2005). Gli2 and Gli3 localize to cilia and require the intraflagellar transport protein polaris for processing and function. *PLoS Genet.* **1**, e53.
He, M., Subramanian, R., Bangs, F., Omelchenko, T., Liem, K. F., Jr, Kapoor, T. M. and Anderson, K. V. (2014). The kinesin-4 protein Kif7 regulates mammalian Hedgehog signalling by organizing the cilium tip compartment. *Nat. Cell Biol.* **16**, 663-672.
Hirokawa, N. (2000). Stirring up development with the heterotrimeric kinesin KIF3. *Traffic* **1**, 29-34.
Hirokawa, N., Noda, Y., Tanaka, Y. and Niwa, S. (2009). Kinesin superfamily motor proteins and intracellular transport. *Nat. Rev. Mol. Cell Biol.* **10**, 682-696.
Hsu, S.-H. C., Zhang, X., Yu, C., Li, Z. J., Wunder, J. S., Hui, C.-C. and Alman, B. A. (2011). Kif7 promotes hedgehog signaling in growth plate chondrocytes by restricting the inhibitory function of Sufu. *Development* **138**, 3791-3801.
Huang, C.-J., Huang, C.-C. and Chang, C.-C. (2012). Association of the testis-specific TRIM/RBCC protein RNF33/TRIM60 with the cytoplasmic motor proteins KIF3A and KIF3B. *Mol. Cell. Biochem.* **360**, 121-131.
Huangfu, D., Liu, A., Rakeman, A. S., Murcia, N. S., Niswander, L. and Anderson, K. V. (2003). Hedgehog signalling in the mouse requires intraflagellar transport proteins. *Nature* **426**, 83-87.
Hui, C.-C. and Angers, S. (2011). Gli proteins in development and disease. *Annu. Rev. Cell Dev. Biol.* **27**, 513-537.
Insinna, C., Pathak, N., Perkins, B. and Drummond, I. (2008). The homodimeric kinesin, Kif17, is essential for vertebrate photoreceptor sensory outer segment development. *Dev Biol.* **316**, 160-170.
Jimbo, T., Kawasaki, Y., Koyama, R., Sato, R., Takada, S., Haraguchi, K. and Akiyama, T. (2002). Identification of a link between the tumour suppressor APC and the kinesin superfamily. *Nat. Cell Biol.* **4**, 323-327.
Keady, B. T., Samtani, R., Tobita, K., Tsuchya, M., San Agustin, J. T., Follit, J. A., Jonassen, J. A., Subramanian, R., Lo, C. W. and Pazour, G. J. (2012). IFT25 links the signal-dependent movement of Hedgehog components to intraflagellar transport. *Dev. Cell* **22**, 940-951.
Kim, J., Kato, M. and Beachy, P. A. (2009). Gli2 trafficking links Hedgehog-dependent activation of Smoothened in the primary cilium to transcriptional activation in the nucleus. *Proc. Natl. Acad. Sci. USA* **106**, 21666-21671.
Kogerman, P., Grimm, T., Kogerman, L., Krause, D., Undén, A. B., Sandstedt, B., Toftgård, R. and Zaphiropoulos, P. G. (1999). Mammalian suppressor-of-fused modulates nuclear-cytoplasmic shuttling of Gli-1. *Nat. Cell Biol.* **1**, 312-319.
Li, Z. J., Nieuwenhuis, E., Nien, W., Zhang, X., Zhang, J., Puviindran, V., Wainwright, B. J., Kim, P. C. W. and Hui, C.-C. (2012). Kif7 regulates Gli2 through Sufu-dependent and -independent functions during skin development and tumorigenesis. *Development* **139**, 4152-4161.
Liem, K. F., Jr, He, M., Ocbina, P. J. R. and Anderson, K. V. (2009). Mouse Kif7/Costal2 is a cilia-associated protein that regulates Sonic hedgehog signaling. *Proc. Natl. Acad. Sci. USA* **106**, 13377-13382.
Liu, A., Wang, B. and Niswander, L. A. (2005). Mouse intraflagellar transport proteins regulate both the activator and repressor functions of Gli transcription factors. *Development* **132**, 3103-3111.
Liu, Y. C., Couzens, A. L., Deshwar, A. R., B McBroom-Cerajewski, L. D., Zhang, X., Puviindran, V., Scott, I. C., Gingras, A.-C., Hui, C.-C. and Angers, S. (2014). The PPFIA1-PP2A protein complex promotes trafficking of Kif7 to the ciliary tip and Hedgehog signaling. *Sci. Signal.* **7**, ra117.
Marigo, V., Davey, R. A., Zuo, Y. and Cunningham, J. M. (1996). Biochemical evidence that patched is the Hedgehog receptor. *Nature* **384**, 176-179.
Marks, S. A. and Kalderon, D. (2011). Regulation of mammalian Gli proteins by Costal 2 and PKA in Drosophila reveals Hedgehog pathway conservation. *Development* **138**, 2533-2542.
Matise, M. P., Epstein, D. J., Park, H. L., Platt, K. A. and Joyner, A. L. (1998). Gli2 is required for induction of floor plate and adjacent cells, but not most ventral neurons in the mouse central nervous system. *Development* **125**, 2759-2770.
Maurya, A. K., Ben, J., Zhao, Z., Lee, R. T. H., Niah, W., Ng, A. S. M., Iyu, A., Yu, W., Elworthy, S., van Eeden, F. J. M. et al. (2013). Positive and negative regulation of Gli activity by Kif7 in the zebrafish embryo. *PLoS Genet.* **9**, e1003955.
McMahon, A. P., Ingham, P. W. and Tabin, C. J. (2003). Developmental roles and clinical significance of hedgehog signaling. *Curr. Top. Dev. Biol.* **53**, 1-114.
Megason, S. G. and McMahon, A. P. (2002). A mitogen gradient of dorsal midline Wnts organizes growth in the CNS. *Development* **129**, 2087-2098.
Meyer, N. P. and Roelink, H. (2003). The amino-terminal region of Gli3 antagonizes the Shh response and acts in dorsoventral fate specification in the developing spinal cord. *Dev. Biol.* **257**, 343-355.
Morris, R. L., English, C. N., Lou, J. E. and Dufort, F. J. (2004). Redistribution of the kinesin-II subunit KAP from cilia to nuclei during the mitotic and ciliogenic cycles in sea urchin embryos. *Dev. Biol.* **33**, 622-634.
Morsci, N. S. and Barr, M. M. (2011). Kinesin-3 KLP-6 regulates intraflagellar transport in male-specific cilia of Caenorhabditis elegans. *Curr. Biol.* **21**, 1239-1244.
Nonaka, S., Tanaka, Y., Okada, Y., Takeda, S., Harada, A., Kanai, Y., Kido, M. and Hirokawa, N. (1998). Randomization of left-right asymmetry due to loss of nodal cilia generating leftward flow of extraembryonic fluid in mice lacking KIF3B motor protein. *Cell* **95**, 829-837.
Norman, R. X., Ko, H. W., Huang, V., Eun, C. M., Abler, L. L., Zhang, Z., Sun, X. and Eggenschwiler, J. T. (2009). Tubby-like protein 3 (TULP3) regulates patterning in the mouse embryo through inhibition of Hedgehog signaling. *Hum. Mol. Genet.* **18**, 1740-1754.
Nozawa, Y. I., Lin, C. and Chuang, P.-T. (2013). Hedgehog signaling from the primary cilium to the nucleus: an emerging picture of ciliary localization, trafficking and transduction. *Curr. Opin. Genet. Dev.* **23**, 429-437.
Nybakken, K., Vokes, S. A., Lin, T.-Y., McMahon, A. P. and Perrimon, N. (2005). A genome-wide RNA interference screen in Drosophila melanogaster cells for new components of the Hh signaling pathway. *Nat. Genet.* **37**, 1323-1332.
Ocbina, P. J. R., Eggenschwiler, J. T., Moskowitz, I. and Anderson, K. V. (2011). Complex interactions between genes controlling trafficking in primary cilia. *Nat. Genet.* **43**, 547-553.
Oosterveen, T., Kurdija, S., Alekseenko, Z., Uhde, C. W., Bergsland, M., Sandberg, M., Andersson, E., Dias, J. M., Muhr, J. and Ericson, J. (2012). Mechanistic differences in the transcriptional interpretation of local and long-range Shh morphogen signaling. *Dev. Cell* **23**, 1006-1019.
Pan, Y., Bai, C. B., Joyner, A. L. and Wang, B. (2006). Sonic hedgehog signaling regulates Gli2 transcriptional activity by suppressing its processing and degradation. *Mol. Cell. Biol.* **26**, 3365-3377.
Pedersen, L. B. and Rosenbaum, J. L. (2008). Intraflagellar transport (IFT) role in ciliary assembly, resorption and signalling. *Curr. Top. Dev. Biol.* **85**, 23-61.
Peterson, K. A., Nishi, Y., Ma, W., Vedenko, A., Shokri, L., Zhang, X., McFarlane, M., Baizabal, J.-M., Junker, J. P., van Oudenaarden, A. et al. (2012). Neural-specific Sox2 input and differential Gli-binding affinity provide context and positional information in Shh-directed neural patterning. *Genes Dev.* **26**, 2802-2816.
Phang, H.-Q., Hoon, J.-L., Lai, S.-K., Zeng, Y., Chiam, K.-H., Li, H.-Y. and Koh, C.-G. (2014). POPX2 phosphatase regulates the KIF3 kinesin motor complex. *J. Cell Sci.* **127**, 727-739.
Qin, H., Diener, D. R., Geimer, S., Cole, D. G. and Rosenbaum, J. L. (2004). Intraflagellar transport (IFT) cargo: IFT transports flagellar precursors to the tip and turnover products to the cell body. *J. Cell Biol.* **164**, 255-266.
Qin, J., Lin, Y., Norman, R. X., Ko, H. W. and Eggenschwiler, J. T. (2011). Intraflagellar transport protein 122 antagonizes Sonic Hedgehog signaling and controls ciliary localization of pathway components. *Proc. Natl. Acad. Sci. USA* **108**, 1456-1461.
Robbins, D. J., Nybakken, K. E., Kobayashi, R. and Sisson, J. C. (1997). Hedgehog elicits signal transduction by means of a large complex containing the kinesin-related protein costal2. *Cell* **90**, 225-234.
Roessler, E., Ermilov, A. N., Grange, D. K., Wang, A., Grachtchouk, M., Dlugosz, A. A. and Muenke, M. (2005). A previously unidentified amino-terminal domain regulates transcriptional activity of wild-type and disease-associated human GLI2. *Hum. Mol. Genet.* **14**, 2181-2188.
Ruiz i Altaba, A. (2011). Hedgehog signaling and the Gli code in stem cells, cancer, and metastases. *Sci. Signal.* **4**, pt9.
Sasaki, H., Nishizaki, Y., Hui, C., Nakafuku, M. and Kondoh, H. (1999). Regulation of Gli2 and Gli3 activities by an amino-terminal repression domain: implication of Gli2 and Gli3 as primary mediators of Shh signaling. *Development* **126**, 3915-3924.
Scholey, J. M. (2003). Intraflagellar transport. *Annu. Rev. Cell Dev. Biol.* **19**, 423-443.
Scholey, J. M. (2013). Kinesin-2: a family of heterotrimeric and homodimeric motors with diverse intracellular transport functions. *Annu. Rev. Cell Dev. Biol.* **29**, 443-469.
Sisson, J. C., Ho, K. S., Suyama, K. and Scott, M. P. (1997). Costal2, a novel kinesin-related protein in the Hedgehog signaling pathway. *Cell* **90**, 235-245.
Snow, J. J., Ou, G., Gunnarson, A. L., Walker, M. R. S., Zhou, H. M., Brust-Mascher, I. and Scholey, J. M. (2004). Two anterograde intraflagellar transport motors cooperate to build sensory cilia on C. elegans neurons. *Nat. Cell Biol.* **6**, 1109-1113.
Stamataki, D., Ulloa, F., Tsoni, S. V., Mynett, A. and Briscoe, J. (2005). A gradient of Gli activity mediates graded Sonic Hedgehog signaling in the neural tube. *Genes Dev.* **19**, 626-641.
Stone, D. M., Hynes, M., Armanini, M., Swanson, T. A., Gu, Q., Johnson, R. L., Scott, M. P., Pennica, D., Goddard, A., Phillips, H. et al. (1996). The tumour-suppressor gene patched encodes a candidate receptor for Sonic hedgehog. *Nature* **384**, 129-134.
Takeda, S., Yonekawa, Y., Tanaka, Y., Okada, Y., Nonaka, S. and Hirokawa, N. (1999). Left-right asymmetry and kinesin superfamily protein KIF3A: new insights in determination of laterality and mesoderm induction by kif3A-/- mice analysis. *J. Cell Biol.* **145**, 825-836.
Tanuma, N., Nomura, M., Ikeda, M., Kasugai, I., Tsubaki, Y., Takagaki, K., Kawamura, T., Yamashita, Y., Sato, I., Sato, M. et al. (2009). Protein phosphatase Dusp26 associates with KIF3 motor and promotes N-cadherin-mediated cell-cell adhesion. *Oncogene* **28**, 752-761.
Teng, J., Rai, T., Tanaka, Y., Takei, Y., Nakata, T., Hirasawa, M., Kulkarni, A. B. and Hirokawa, N. (2005). The KIF3 motor transports N-cadherin and organizes the developing neuroepithelium. *Nat. Cell Biol.* **7**, 474-482.

Tukachinsky, H., Lopez, L. V. and Salic, A. (2010). A mechanism for vertebrate Hedgehog signaling: recruitment to cilia and dissociation of SuFu-Gli protein complexes. *J. Cell Biol.* **191**, 415-428.
Vokes, S. A., Ji, H., McCuine, S., Tenzen, T., Giles, S., Zhong, S., Longabaugh, W. J. R., Davidson, E. H., Wong, W. H. and McMahon, A. P. (2007). Genomic characterization of Gli-activator targets in sonic hedgehog-mediated neural patterning. *Development* **134**, 1977-1989.
Wang, B., Fallon, J. F. and Beachy, P. A. (2000). Hedgehog-regulated processing of Gli3 produces an anterior/posterior repressor gradient in the developing vertebrate limb. *Cell* **100**, 423-434.
Wang, C., Pan, Y. and Wang, B. (2010). Suppressor of fused and Spop regulate the stability, processing and function of Gli2 and Gli3 full-length activators but not their repressors. *Development* **137**, 2001-2009.
Wedaman, K. P., Meyer, D. W., Rashid, D. J., Cole, D. G. and Scholey, J. M. (1996). Sequence and submolecular localization of the 115-kD accessory subunit of the heterotrimeric kinesin-II (KRP85/95) complex. *J. Cell Biol.* **132**, 371-380.
Wen, X., Lai, C. K., Evangelista, M., Hongo, J. A., de Sauvage, F. J. and Scales, S. J. (2010). Kinetics of hedgehog-dependent full-length Gli3 accumulation in primary cilia and subsequent degradation. *Mol. Cell. Biol.* **30**, 1910-1922.
Yamazaki, H., Nakata, T., Okada, Y. and Hirokawa, N. (1995). KIF3A/B: a heterodimeric kinesin superfamily protein that works as a microtubule plus end-directed motor for membrane organelle transport. *J. Cell Biol.* **130**, 1387-1399.
Yamazaki, H., Nakata, T., Okada, Y. and Hirokawa, N. (1996). Cloning and characterization of KAP3: a novel kinesin superfamily-associated protein of KIF3A/3B. *Proc. Natl. Acad. Sci. USA* **93**, 8443-8448.
Yang, Z. and Goldstein, L. S. (1998). Characterization of the KIF3C neural kinesin-like motor from mouse. *Mol. Biol. Cell* **9**, 249-261.
Yang, Z., Roberts, E. A. and Goldstein, L. S. (2001). Functional analysis of mouse kinesin motor Kif3C. *Mol. Cell. Biol.* **21**, 5306-5311.

Journal of Cell Science